GALCIT REPORT NO. 61-15

GUGGENHEIM AERONAUTICAL LABORATORY

CALIFORNIA INSTITUTE OF TECHNOLOGY

REPORT_____

PASADENA, CALIFORNIA

FORM AL-5 3M 7-56

FUNDAMENTAL STUDIES RELATING TO THE MECHANICAL BEHAVIOR OF SOLID PROPELLANTS, ROCKET GRAINS AND ROCKET MOTORS

GALCIT SM 61-15

GALCIT 118 - PROGRESS REPORT NO. 1

Aerojet Contract S-416394-OP

April 11, 1961 - June 30, 1961

FUNDAMENTAL STUDIES RELATING TO THE MECHANICAL BEHAVIOR OF SOLID PROPELLANTS, ROCKET GRAINS AND ROCKET MOTORS

P. J. Blatz

W. L. Ko

A. Zak

June 1961

This program is being supported by the Aerojet-General Corporation, Sacramento Division, under technical cognizance of Dr. F. J. Climent to provide technical support to the Polaris Project

Guggenheim Aeronautical Laboratory

California Institute of Technology

Pasadena, California

FOREWORD

During the past three years, the mechanical testing of solid propellants, solid rocket grains, and solid rocket motors under idealized conditions has been receiving increased attention. Today it is not uncommon to see a multitude of new techniques and analyses being investigated. One may expect to see dummy propellant prepared with glass bead filler to observe its dilatation to rupture; to ink circles, rectangular grids at various critical areas on a grain surface, and to observe the distortion of these grids as a result of thermal cycling and/or slump; to subject rectangular parallel-opipedal-shaped specimens to both torsion and biaxial tension as well as hydrostatic compression and parallel-plate tension; to apply theories of large elastic strain, and non-linear viscoelasticity; to search for an isotropic failure criterion as well as a crack propagation criterion. In short the mechanics of propellant behavior from small deformation all the way to fracture initiation and propagation has become quite sophisticated. Gradually the results of this testing and their thinking are being integrated in a logical scheme of analysis which is being passed along to the engineer and being used in predicting performance of rocket motors.

This particular program will pertain to four areas:

1) The characterization of polyurethane propellant behavior out to fracture initiation in terms of large strain theory.
2) The development of a failure criterion and crack propagation criteria for said materials.
3) The generation, where possible, of macroscopic mechanical parameters in terms of molecular parameters.
4) The solution of certain stress problems, in both linear and non-linear theory, which are prerequisite to engineering applications.

As such it is part of a continuing research study of structural integrity problems in solid propellant rocket motors being conducted under the general direction of Dr. M. L. Williams in the Guggenheim Aeronautical Laboratory.

This preliminary report is intended as an interim working document to be circulated for the purpose of stimulating discussion.

TABLE OF CONTENTS *

* The contents of this quarterly progress report comprise only Chapters I and IV. Material for the other chapters will be included in subsequent reports also to be organized as indicated.

I. MECHANICAL BEHAVIOR OF RUBBERY MATERIALS

A. Introduction

The term rubbery materials includes both foams and filled rubbers (which may be propellants) as well as continuum rubbers. Experience dictates that the mechanical behavior of foams and filled rubbers (up to 90 percent by weight solids loading) is controlled mainly by the mechanical properties of the rubber binder, and for this reason, it is prudent to start this investigation with a review of the known behavior of rubbery materials.

One typical feature of rubbery or hyper-elastic materials is high extensibility under relatively small load. The deformations are so large (ultimate extension ranges from 500 percent to 1000 percent) that the classical theory of small strain is no longer adequate to express the behavior of such materials. The modern approach initiated by Rivlin, Murnaghan, et al, is to find a strain-energy function from which the constitutive stress-strain law can be established.

For a homogeneous, isotropic elastomeric continuum, the work done in deformation which is stored as strain energy, depends only on certain invariant characteristics of the state of deformation. These invariants in turn are functions only of the proper or diagonal values of the deformation tensor. The purpose of this introduction is to present experimental data on a number of rubbers and show how, from these data one can determine the relation of the strain energy function to the invariants of the deformation state.

Obviously the algebra involved in effecting this data reduction is simplified in the case of homogeneous deformations. For this reason, specimens were tested in uniaxial tension and biaxial tension. Data were procured on

a) SBR - 1500 rubber (1.75 % S)
b) Polyurethane foam rubber (47 % by volume voids - 40μ dia.)
c) SBR - 1500 rubber (3 % S)

B. Theory of Large Homogeneous Strains

For homogeneous deformations, it is convenient to define three invariants as follows:

$$J_1 = I_1 = \lambda_i^2 + \lambda_j^2 + \lambda_k^2 \qquad (I.1)$$

$$J_2 = \frac{I_2}{I_3} = \frac{1}{\lambda_i^2} + \frac{1}{\lambda_j^2} + \frac{1}{\lambda^2_k} \qquad (I.2)$$

$$J_3 = \sqrt{I_3} = \lambda_i \lambda_j \lambda_k = \frac{V}{V_o} \qquad (I.3)$$

where the invariants $\{ I_1 , I_2 , I_3 \}$ are the set originally used by Rivlin. Setting $\frac{\partial W}{\partial J_i} \equiv W_i$, the constitutive law reduces to:

$$\sigma_i \lambda_i = \overline{\sigma}_i J_3 = 2 \left[W_1 \lambda_i^2 - \frac{W_2}{\lambda_i^2} \right] + J_3 W_3 , \quad i = 1, 2, 3 \qquad (I.4)$$

where σ_i are the homogeneous components of the engineering stress (load on undeformed cross-section)

$\overline{\sigma}_i$ are the homogeneous components of the true stress

λ_i are the homogeneous components of the deformation gradients (new length / unstretched length)

W is the strain energy / unit volume undeformed material.

For simple tension, the deformation-stress field is defined as:

$$\lambda_i = \lambda , \quad \lambda_j = \lambda_k = \lambda_{lat} , \quad J_3 = \lambda \lambda_{lat}^2 \qquad (I.5)$$

$$\sigma_i = \sigma_{uni} , \quad \sigma_j = \sigma_k = 0 \qquad (I.6)$$

where λ is the logitudinal extension ratio

λ_{lat} is the lateral contraction ratio

Substitution into (I. 4) yields:

$$\sigma_{uni} \lambda = 2 \left[W_1 \lambda^2 - \frac{W_2}{\lambda^2} \right] + \lambda \lambda_{lat}^2 W_3 \qquad (I.7)$$

$$0 = 2 \left[W_1 \lambda_{lat}^2 - \frac{W}{\lambda_{lat}^2} \right] + \lambda \lambda_{lat}^2 W_3 \qquad (I.8)$$

W_3 may be eliminated by subtraction:

$$\frac{\sigma_{uni}\,\lambda}{\lambda^2-\lambda^2_{lat}} = 2\left[W_1 + \frac{W_2}{\lambda^2\lambda^2_{lat}}\right] \qquad (I.9)$$

Assuming W_1 and W_2 are constant, a plot of $\sigma_{uni}\lambda/(\lambda^2 - \lambda^2_{lat})$ vs $1/\lambda^2\lambda^2_{lat}$ may be used to determine these material parameters.

For biaxial tension, the deformation-stress field is defined as:

$$\lambda_i = \lambda\,, \quad \lambda_j = 1\,, \quad \lambda_k = \lambda_{th}\,, \quad J_3 = \lambda\lambda_{th} \qquad (I.10)$$

$$\sigma_i = \sigma_{bi}\,, \quad \sigma_j = \sigma_{lat}\,, \quad \sigma_k = 0$$

where λ_{th} is the thickness contraction ratio

σ_{lat} is the lateral stress applied to maintain constant width.

Substitution into (I. 4) yields:

$$\sigma_{bi}\lambda = 2\left[W_1\lambda^2 - \frac{W_2}{\lambda^2}\right] + \lambda\lambda_{th}W_3 \qquad (I.11)$$

$$0 = 2\left[W_1\lambda^2_{th} - \frac{W_2}{\lambda^2_{th}}\right] + \lambda\lambda_{th}W_3 \qquad (I.12)$$

Again W_3 is eliminated by subtraction:

$$\frac{\sigma_{bi}\,\lambda}{\lambda^2-\lambda^2_{th}} = 2\left[W_1 + \frac{W_2}{\lambda^2\lambda^2_{th}}\right] \qquad (I.13)$$

Again (I. 13) may be plotted to fit the assumption that W_1 and W_2 are constants. Actually, constancy of the left hand members of (I. 9) alone is insufficient to guarantee that W_1 and W_2 are constants, since they could vary in such a way to maintain the right-hand member constant. For this reason a double check is needed and is provided by the type of biaxial test described in (I. 11) and (I. 12).

We can anticipate two simple types of results:

a) $W_2 = 0$, W_1 = constant = $\frac{\mu}{2}$ (by comparison with linear theory)

b) $W_2 = W_1$ = constant

In the case a), it follows that:

$$W_{13} = 0 \qquad (I.14)$$

$$W_3 = W_3(J_3) \text{ independent of } J_1 \qquad (I.15)$$

For this case, (I.4) becomes:

$$\sigma_i \lambda_i = \overline{\sigma}_i J_3 = \mu \lambda_i^2 + J_3 W_3 \qquad (I.16)$$

And from comparison with linear theory, the character of the leading terms in the expansion of $J_3 W_3$ is established to be:

$$J_3 W_3 = -\mu + \left(K - \frac{2}{3}\mu\right)(J_3 - 1) + C(J_3 - 1)^2 + \cdots \qquad (I.17)$$

It will be important to establish the radius of convergence of the entire section which this power series represents analytically. For, if it turns out that

a) the ultimate dilatation J_3^* falls within the circle of convergence, and

b) $C(J_3^* - 1)^2 << \left(K - \frac{2}{3}\mu\right)(J_3^* - 1)$, then a very useful constitutive equation develops, namely:

$$\overline{\sigma}_i J_3 = \sigma_i \lambda_i = \mu(\lambda_i^2 - 1) + \left(K - \frac{2}{3}\mu\right)(J_3 - 1) \qquad (I.18)$$

Consider now the case in which both W_1 and W_2 are constant:

$$W_1 = \frac{\mu}{2} f \qquad (I.19)$$

$$W_2 = \frac{\mu}{2}(1 - f) \qquad (I.20)$$

$$W_{13} = W_{23} = 0 \qquad (I.21)$$

$$W_3 = W_3(J_3) \qquad \text{independent of } J_1 \text{ and } J_2 \qquad (I.22)$$

For this case, (I.4) becomes:

$$\sigma_i \lambda_i = \bar{\sigma}_i J_3 = \mu \left[f \lambda_i^2 + \frac{1-f}{\lambda_i^2} \right] + J_3 W_3 \qquad \text{I.23}$$

Before continuing, let us check the theory to this point.

C. Experimental Adductions to the Theory as Developed

1. Materials tested or to be tested

a. Polyurethane Foam Rubber (47 % void)

Composition: PPG:MTDA:TDI = 70:30:107

The polyurethane elastomer was filled with 47% by volume of water-soluble sodium-chloride-salt and then casted. The foam was obtained by extracting the salt with boiling water, then dried. The average diameter of the holes is 40 μ .

b. SBR-1500(1.75% Sulfur) = cured at 307°F for 45 min.
c. SBR-1500(3% Sulfur) = cured at 307°F for 45 min.
d. Natural Rubber(2% Sulfur)= cured at 307°F for 20 min.
e. Natural Rubber(4% Sulfur)= cured at 307°F for 20 min.
f. Cis - 4 = cured at 307°F for 20 min.
g. Paracril B = cured at 307°F for 45 min.
h. Neoprene - GNA = cured at 307°F for 20 min.
i. Butyl-217 = cured at 307°F for 45 min.

The materials from (b) to (i) were cured from the gum stocks at 307°F in a hot-press-mold for certain cure-time as shown above, then the mold which contains a specimen was removed from the press and cooled in the atmosphere.

2. Specimen Geometries

a. Uniaxial Tensile Test Specimens:

As shown in the sketch (cf. Figure I.1) two types of test specimens were used. The working length remains the same (ℓ = 5") for both types of specimen, and w = 1" for type I, w = 1/2" for type II respectively. The thickness t for each test is listed on Table I.1 .

In order to reduce the end effect both sides of both ends of a specimen were glued on thin aluminum sheets. The metal sheets (or blocks)

which are thinner than the specimen were put in between the metal sheets to protect the ends from being squeezed too far when gripped. It is especially good for a foam rubber specimen.

The markings were made at the middle edges of the specimen by ink.

b. Biaxial Tensile Test Specimens:

The working length for this case is $\ell = 1''$ for Type I and $\ell = 1/2''$ for Type II, (and $w \gg \ell \gg t$) as shown in Figure I.2. The thickness t and width w for each test are listed on Table I.1 .

A thin sheet of specimen is glued both sides of both ends on thin steel plates to prevent the lateral contraction.

The markings were made at the middle edges of the working length.

3. Test Procedures

All the test specimens were prestressed at constant temperature up to 40% $\sim$ 50% elongation few times to eliminate hysteresis. In order to read λ_{lat} or λ_{th} corresponding to the equilibrium state in uniaxial and biaxial tension, the crosshead was stopped and the chart allowed to continue on until the load-time curve leveled off. For every λ, the corresponding λ_{lat} , λ_{th} were then measured to 10^{-4} in. accuracy. In uniaxial tension, for extensions up to 1", the measurements of λ_{lat} were made for every 0.25" interval of extension, and beyond that every 0.5" interval. In biaxial tension, λ_{th} were measured for every 0.1" interval.

From the test data the following curves were plotted (cf Figures 3 $\sim$ 26):

i) σ_{uni} v.s. λ , σ_{bi} v.s. λ

ii) $\dfrac{\sigma_{uni}\lambda}{\lambda^2-\lambda_{lat}^2}$ v.s. $\dfrac{1}{\lambda^2\lambda_{lat}^2}$, $\dfrac{\sigma_{bi}\lambda}{\lambda^2-\lambda_{th}^2}$ v.s. $\dfrac{1}{\lambda^2\lambda_{th}^2}$

iii) λ_{lat} v.s. λ , λ_{th} v.s. λ

iv) $J_3(=\lambda\lambda_{lat}^2)$ v.s. λ , $J_3(=\lambda\lambda_{th})$ v.s. λ

4. Results and Discussion

A complete set of derived information obtained from Figures 3 ~ 26 is shown in Table I. We note the following:

a) W_1 and W_2 are both non-zero, positive constants for both continuum rubbers and foam.

b) The continuum rubber dilates enormously in biaxial tension.

c) The foam's behavior in biaxial is comparable to its behavior in uniaxial tension.

Since item b) is an unusual but not unexpected feature of rubber, hitherto unreported in the open literature, we plan to procure more biaxial data to double check this result. Following this an effective value of Poisson's ratio will be determined, using (I. 18). A complete discussion of this and the isotropic failure criterion will be presented in the following quarterly.

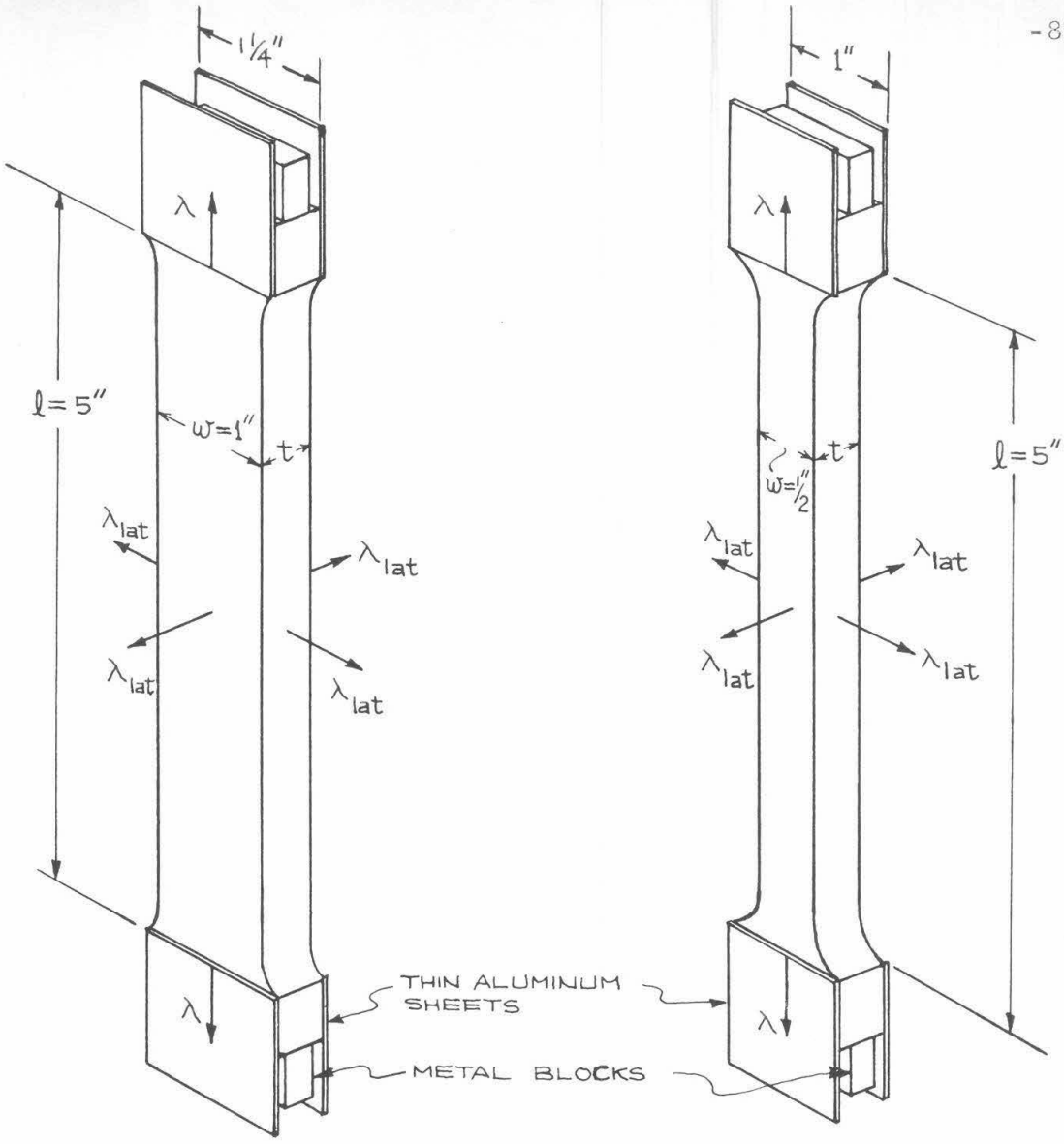

TYPE I

TYPE II

DIMENSIONS t ARE LISTED ON TABLE I.1

FIG. I.1. UNIAXIAL TENSILE TEST SPECIMENS

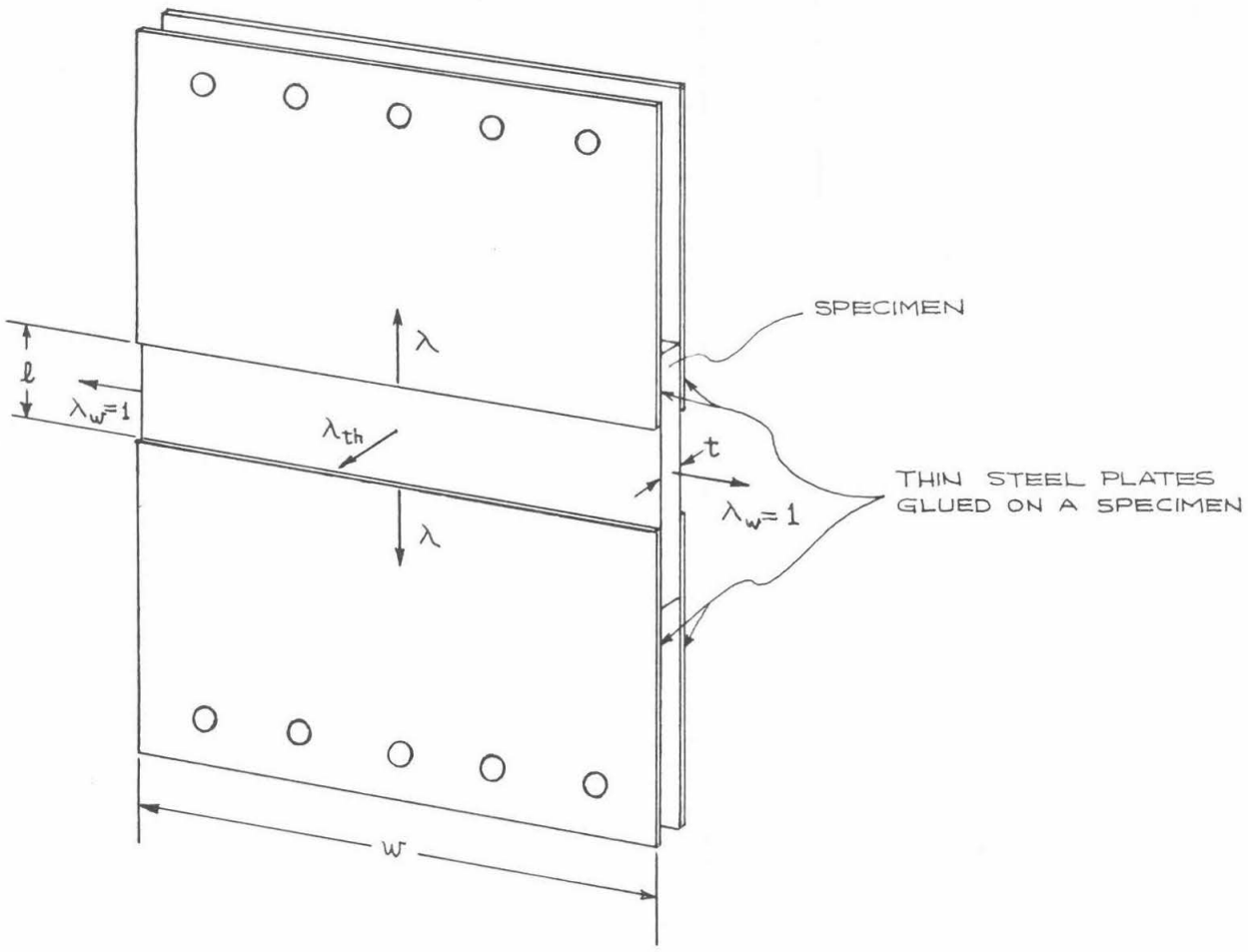

TYPE I : $\ell = 1''$, w AND t ARE LISTED ON TABLE I.1

TYPE II : $\ell = \frac{1}{2}''$, ,,

FIG. I. 2. BIAXIAL TENSILE TEST SPECIMEN

TABLE I.1. LIST OF EXPERIMENTAL RESULTS

MATERIALS	SBR-1500 (1.75% S)		SBR-1500 (1.75% S)		PU FOAM (47% VOID)		PU FOAM (47% VOID)	
SAMPLE DIMENSIONS $\ell \times w \times t$ $\ell : w : t$	$320/64 \times 64/64 \times 5/64$ 64 : 12.8 : 1		$320/64 \times 32/64 \times 5/64$ 64 : 6.4 : 1		$40/8 \times 8/8 \times 3/8$ 13.3 : 2.7 : 1		$40/8 \times 4/8 \times 3/8$ 13.3 : 1.3 : 1	
AMBIENT TEMPERATURE °F	75		75		75		75	
	75	75	75	75	75		75	
σ^*_{uni}, psi.	107.2		100.5		24.0		25.5	
	107.0	115.0	96.9		30.5		30.5	
λ^*	2.15		2.40		1.90		2.00	
	2.23	2.60	2.20		2.34		2.40	
λ^*_{lat}	0.678		0.665		0.865		0.854	
	0.657	0.598	0.682		0.818		0.816	
$J_3^* (= \lambda \lambda_{lat}^2)$	0.990		1.020		1.420		1.460	
	0.992	0.931	1.020		1.565		1.598	
W^*, $\frac{in-lbs}{in^3}$	78.5		85.7		14.2		17.6	
	82.2	115.6	73.0		28.8		32.8	
W_1, psi.	17		14		3.0		2.9	
	17	12	16		3.2		3.0	
W_2, psi.	23		22		13.3		14.8	
	20	27	19		15.8		15.2	
μ, psi.	80		72		32.6		35.4	
	74	78	70		37.6		36.8	
$dJ_3/d\lambda$	0		0		0.474		0.471	
	0	0	0		0.462		0.452	
BIAXIAL TENSION								
SAMPLE DIMENSIONS $\ell \times w \times t$ $\ell : w : t$	$64/64 \times 340/64 \times 5/64$ 12.8 : 68 : 1		$32/64 \times 340/64 \times 5/64$ 6.4 : 68 : 1		$8/8 \times 51/8 \times 3/8$ 2.7 : 17 : 1		$16/16 \times 102/16 \times 3/16$ 5.3 : 34 : 1	
AMBIENT TEMPERATURE °F	75		75		75		76	
	75	75	75		78		76	
σ^*_{bi}, psi.	114.4		101.7		22.6		19.7	
	115.7	100.8	113.2		18.5		24.1	
λ^*	2.20		1.90		2.10		2.10	
	2.00	2.00	2.40		2.10		2.10	
λ^*_{th}	0.650		0.741		0.848		0.850	
	0.749	0.700	0.652		0.891		0.813	
$J_3^* (= \lambda \lambda_{th})$	1.43		1.41		1.78		1.79	
	1.50	1.40	1.56		1.87		1.71	
W^*, $\frac{in-lbs}{in^3}$	86.0		57.2		19.2		16.0	
	72.7	61.7	104.0		17.2		19.1	
W_1, psi.	16		13		3		1.5	
	13	16	11		2		2.5	
W_2, psi.	34		35		14		13.5	
	47	25	36		14		13.0	
μ, psi.	86		92		34		30	
	118	82	94		32		31	
$dJ_3/d\lambda$	0.421		0.457		0.75		0.70	
	0.525	0.400	0.459		0.73		0.65	

TABLE I.1. LIST OF EXPERIMENTAL RESULTS (CONT'D.)

UNIAXIAL TENSION				
MATERIALS	SBR-1500 (3 % S)	SBR-1500 (3 % S)		
SAMPLE DIMENSIONS $\ell \times w \times t$ $\ell : w : t$	$320/64 \times 64/64 \times 5/64$ 64 : 12.8 : 1	$320/64 \times 32/64 \times 5/64$ 64 : 6.4 : 1		
AMBIENT TEMPERATURE °F	77 77	76 77		
σ^*_{uni}, psi.	129.0 118.0	120.0 129.8		
λ^*	2.00 2.00	2.00 2.00		
λ^*_{lat}	0.698 0.730	0.711 0.711		
$J_3^* (= \lambda \lambda_{lat}^2)$	0.975 1.05	1.01 1.01		
W^*, $\frac{in-lbs}{in^3}$	79.1 74.1	77.4 78.5		
W_1, psi.	26 22	19 24		
W_2, psi.	21 24	31 25		
μ, psi.	94 92	100 98		
$dJ_3/d\lambda$	0 0	0 0		
BIAXIAL TENSION				
SAMPLE DIMENSIONS $\ell \times w \times t$ $\ell : w : t$	$64/64 \times 340/64 \times 5/64$ 12.8 : 68 : 1	$32/64 \times 340/64 \times 5/64$ 6.4 : 68 : 1		
AMBIENT TEMPERATURE °F	76 76	77 77		
σ^*_{bi}, psi.	103.2 96.5	127.3 110.0		
λ^*	1.7 1.5	1.7 1.7		
λ^*_{th}	0.776 0.814	0.804 0.804		
$J_3^* (= \lambda \lambda_{th})$	1.32 1.22	1.370 1.370		
W^*, $\frac{in-lbs}{in^3}$	44.2 28.2	51.5 48.1		
W_1, psi.	21 13	15 15		
W_2, psi.	30 52	51 59		
μ, psi.	102 130	148 132		
$dJ_3/d\lambda$	0.45 0.51	0.58 0.58		

FIG. I. 3. UNIAXIAL STRESS V.S. LONGITUDINAL EXTENSION RATIO

SBR-1500 (1.75% S)

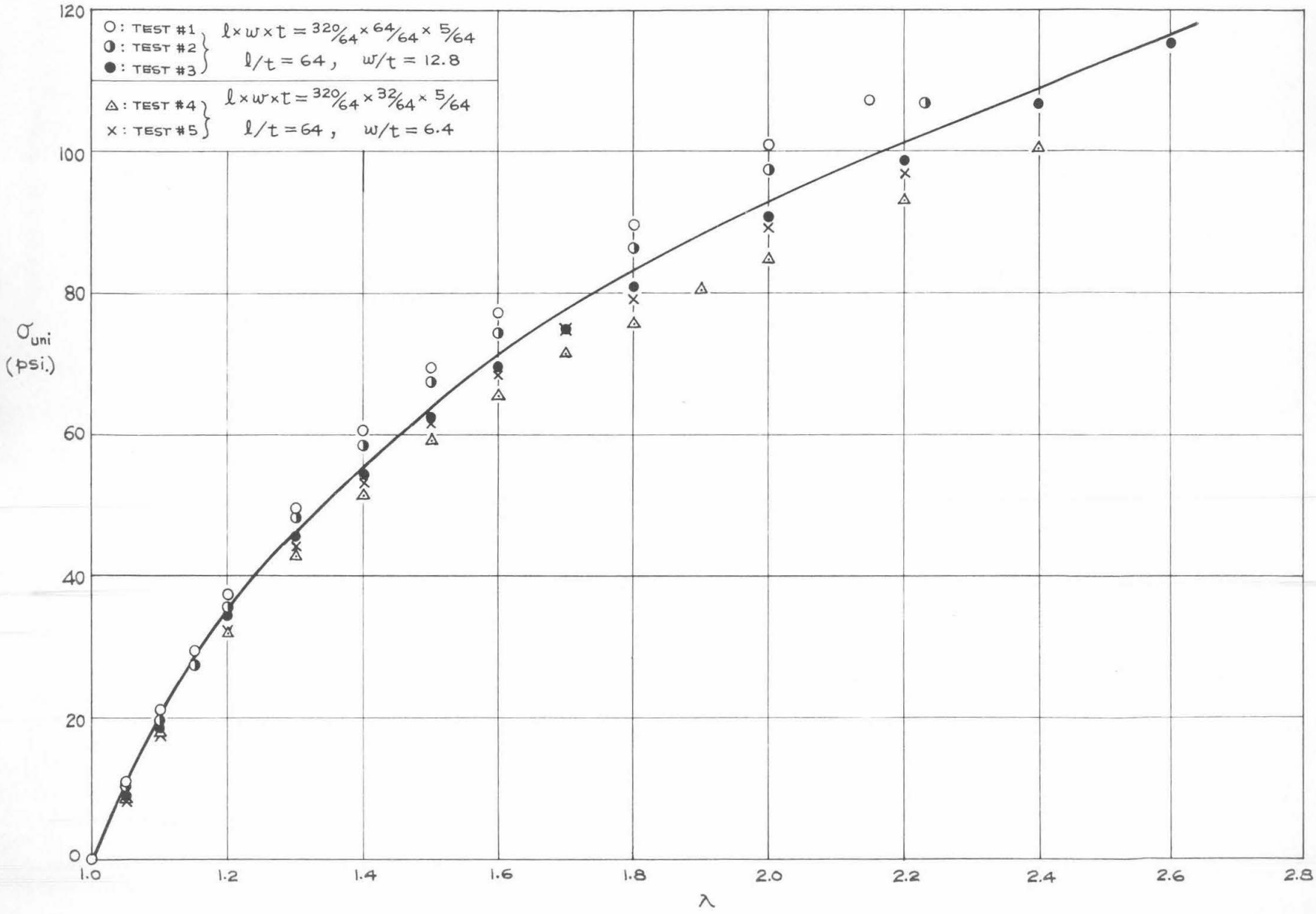

FIG. I. 4. EVALUATION OF W_1 & W_2 FROM RECTIFIED UNIAXIAL DATA

SBR - 1500 (1.75% S)

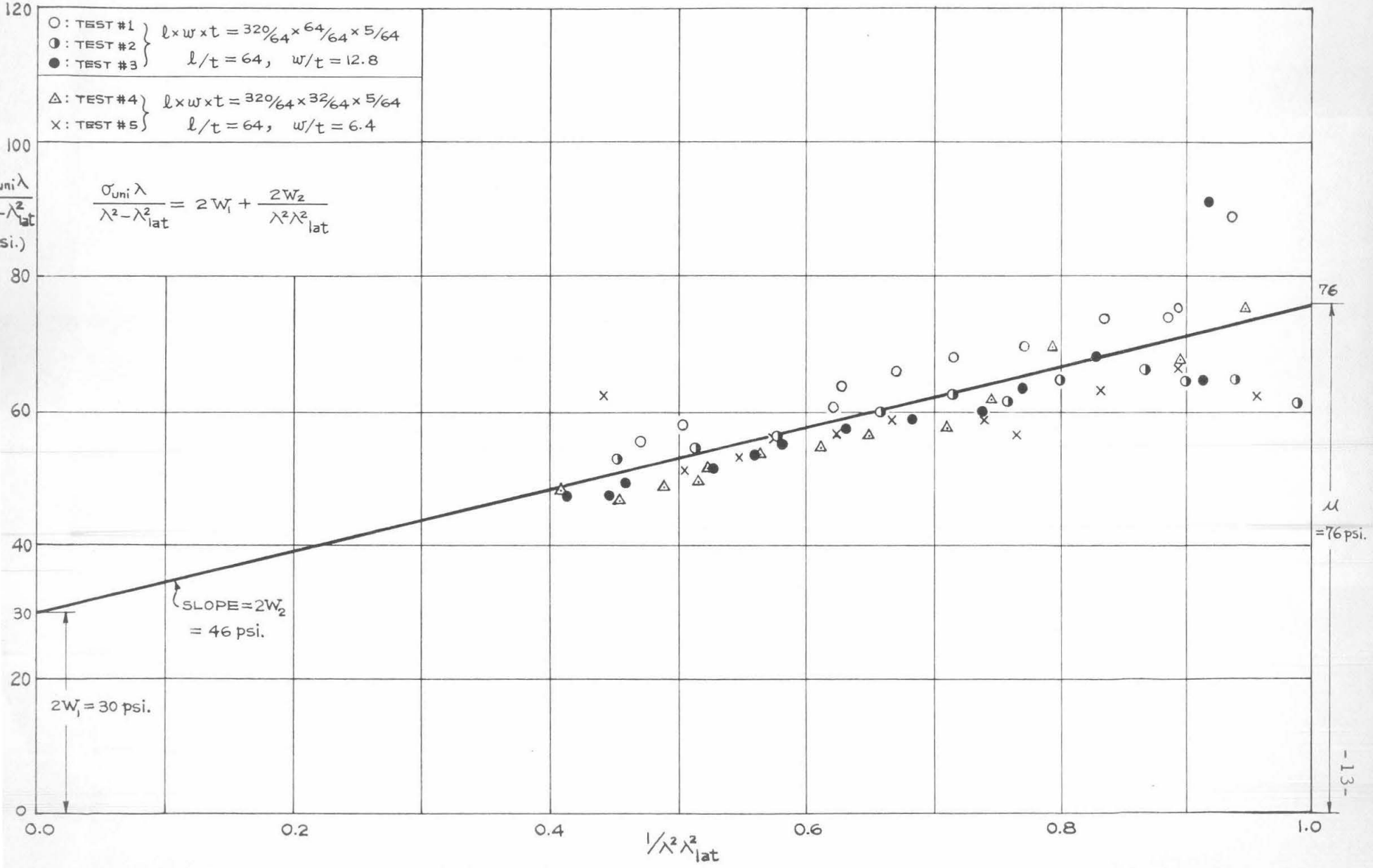

FIG. I. 5. UNIAXIAL LATERAL CONTRACTION RATIO V.S. LONGITUDINAL EXTENSION RATIO

SBR - 1500 (1.75 % S)

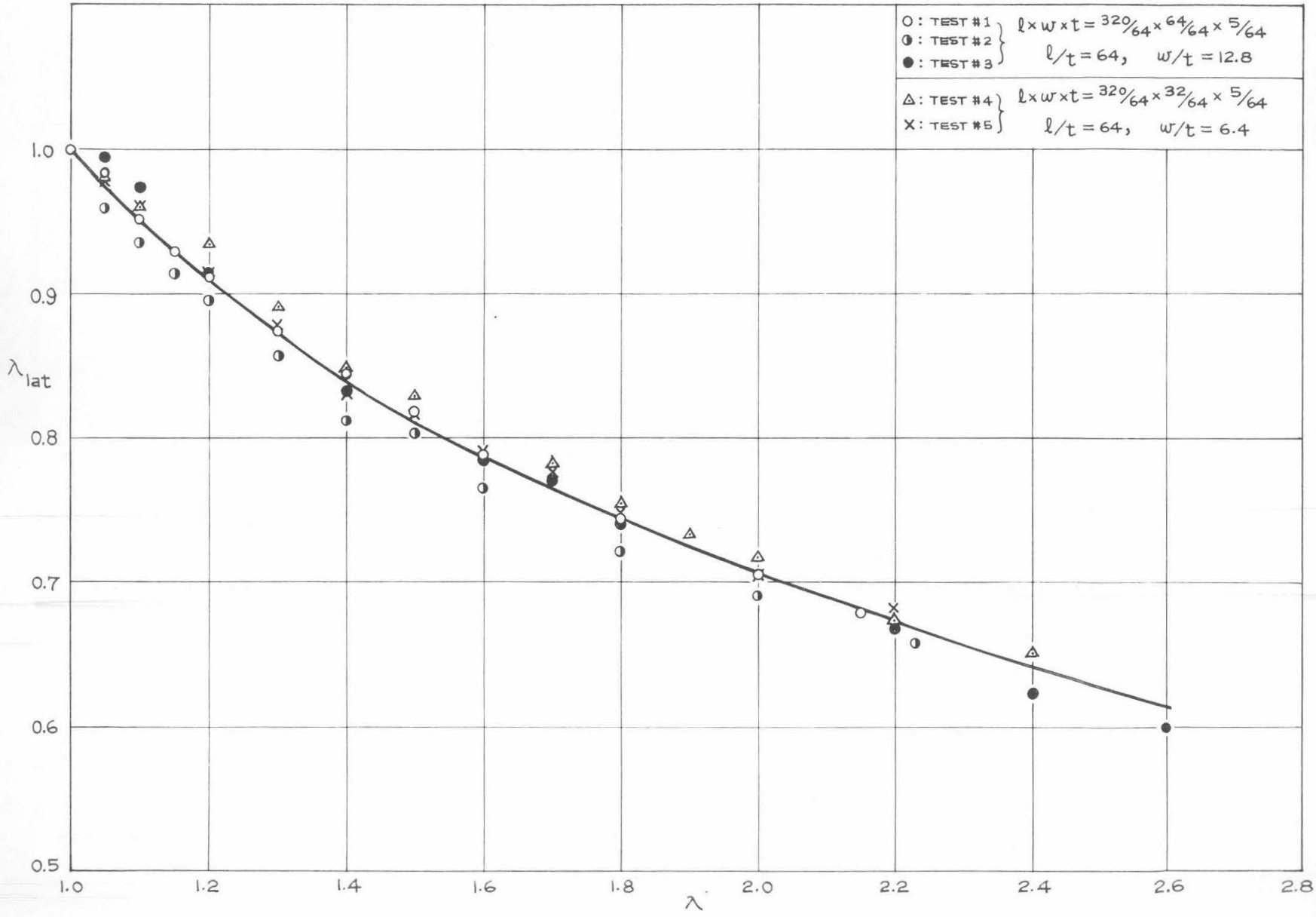

FIG. I. 6. UNIAXIAL DILATATION V.S. LONGITUDINAL EXTENTION RATIO

SBR-1500 (1.75% S)

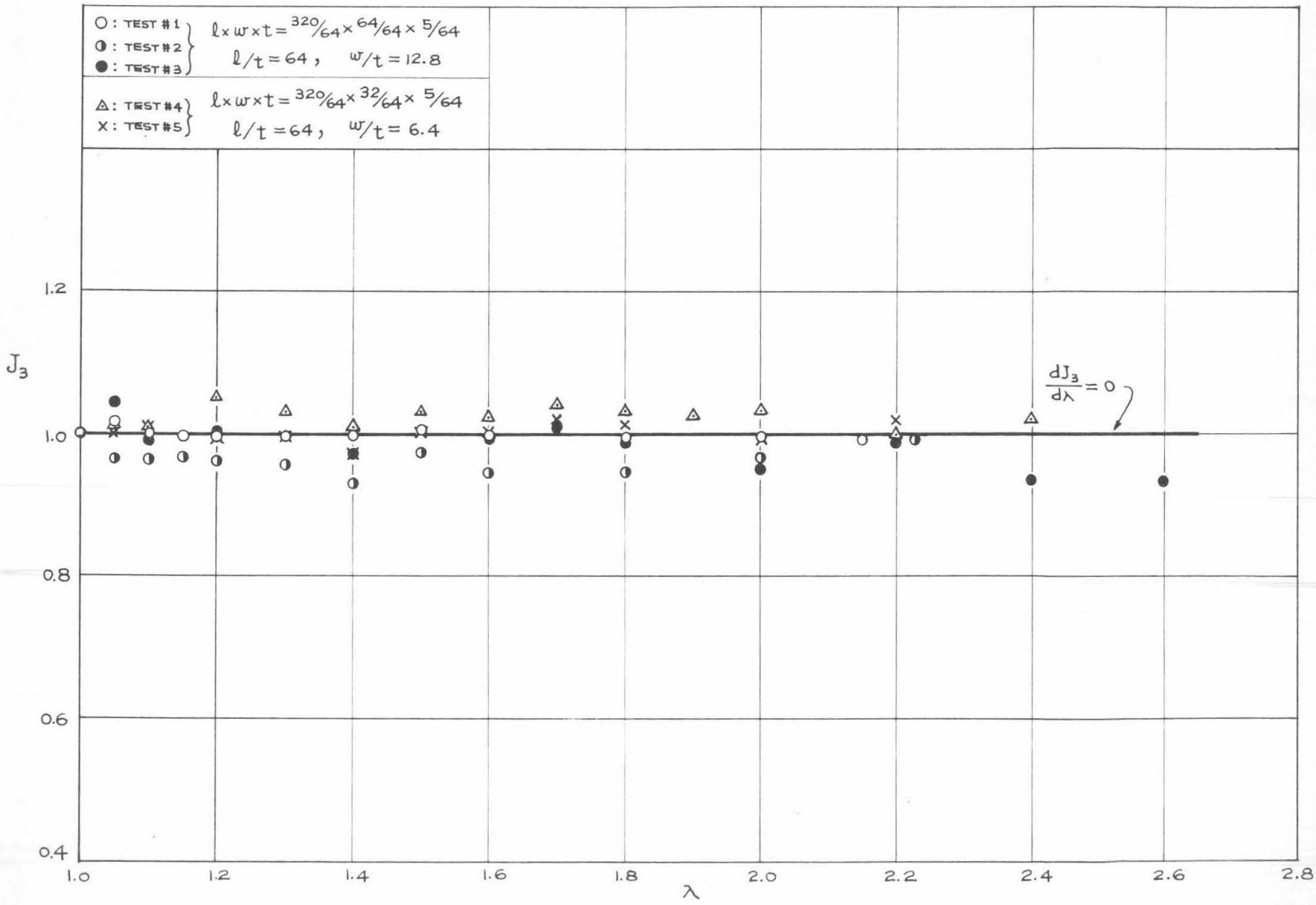

FIG. I. 7. BIAXIAL STRESS V.S. LONGITUDINAL EXTENSION RATIO

SBR-1500 (1.75% S)

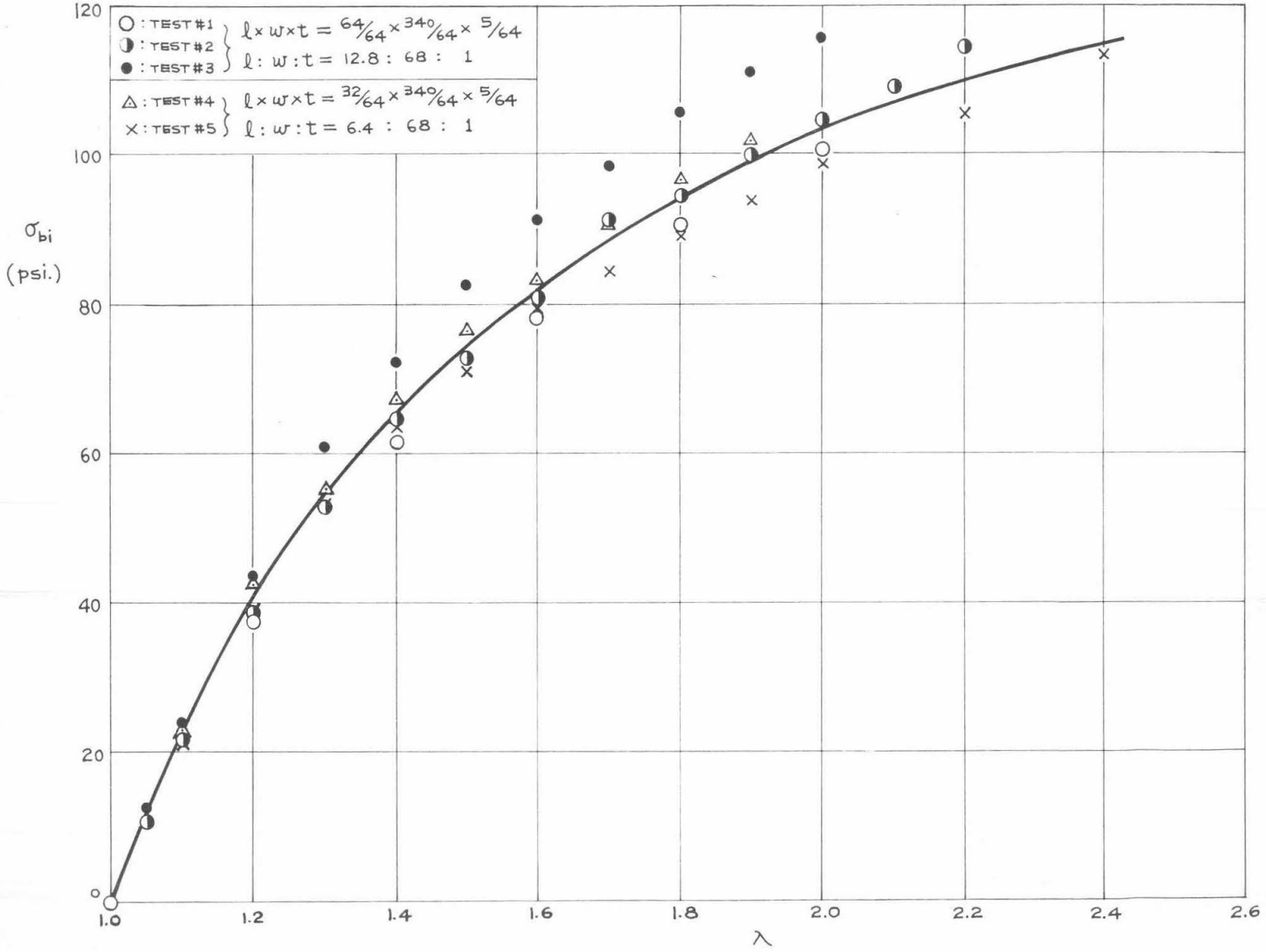

FIG. I. 8. EVALUATION OF W_1 & W_2 FROM RECTIFIED BIAXIAL DATA

SBR-1500 (1.75% S)

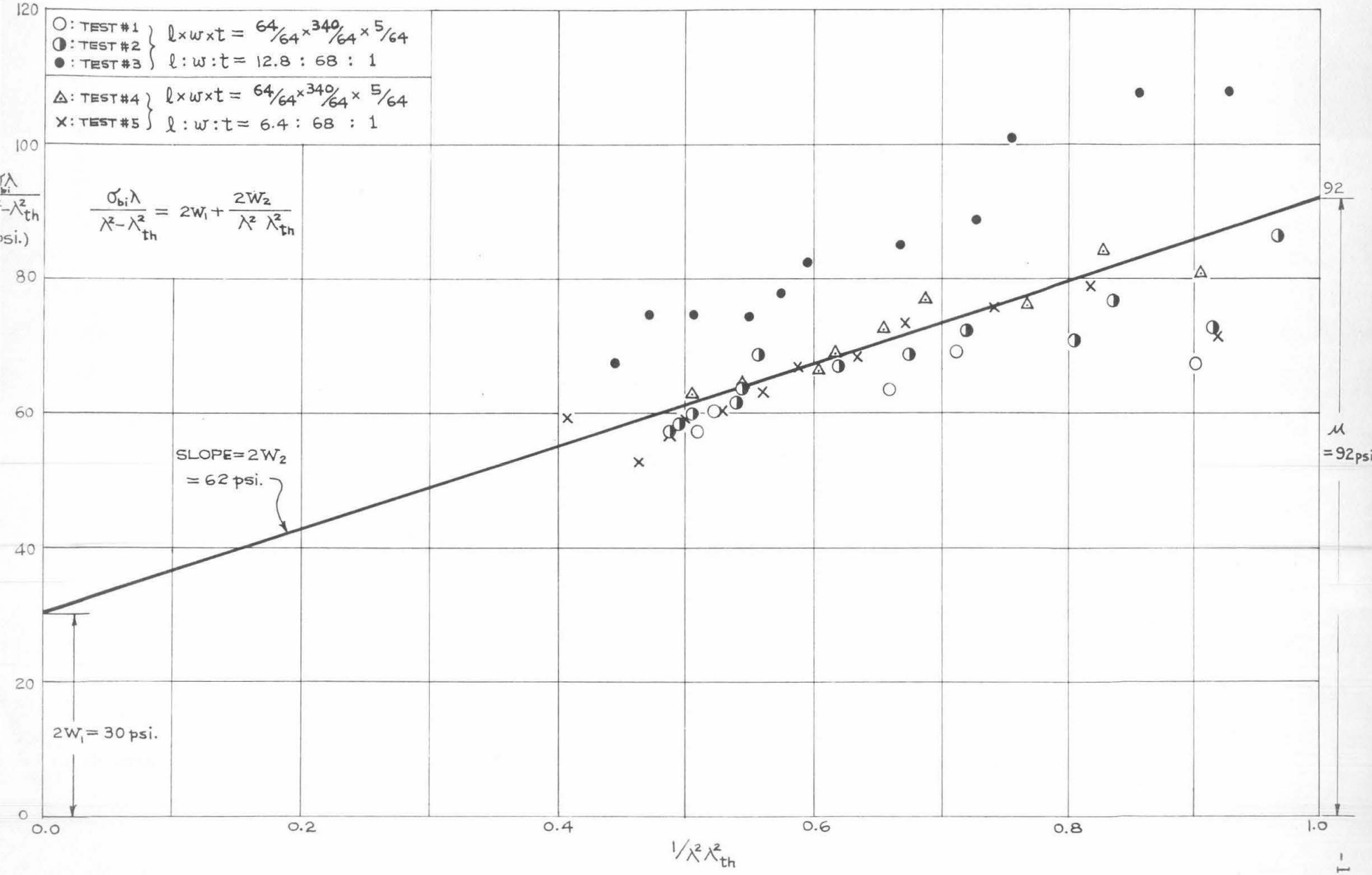

FIG. I. 9. BIAXIAL THICKNESS CONTRACTION RATIO V.S. LONGITUDINAL EXTENSION RATIO

SBR-1500 (1.75% S)

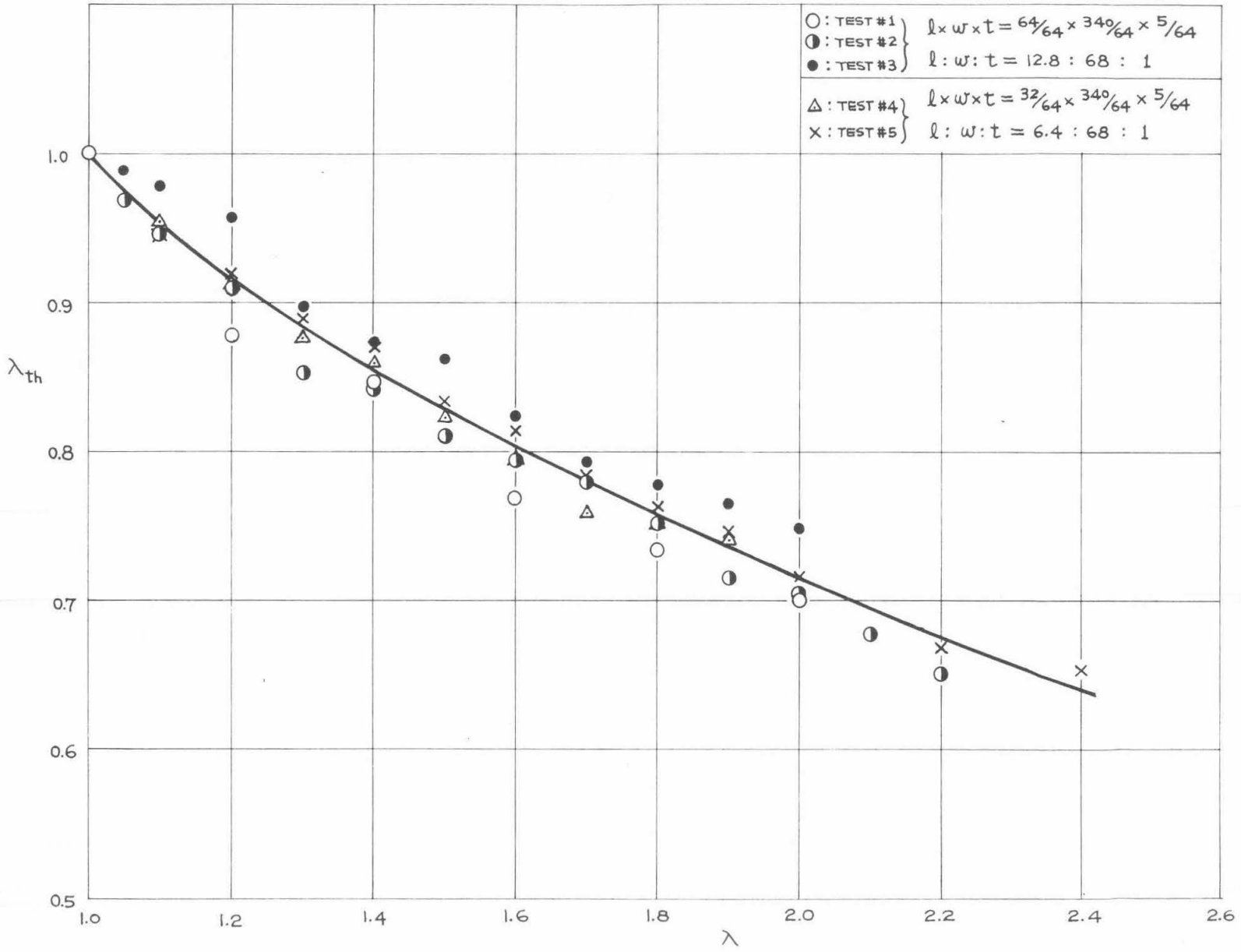

FIG. I. 10. BIAXIAL DILATATION V.S. LONGITUDINAL EXTENSION RATIO

SBR-1500 (1.75% S)

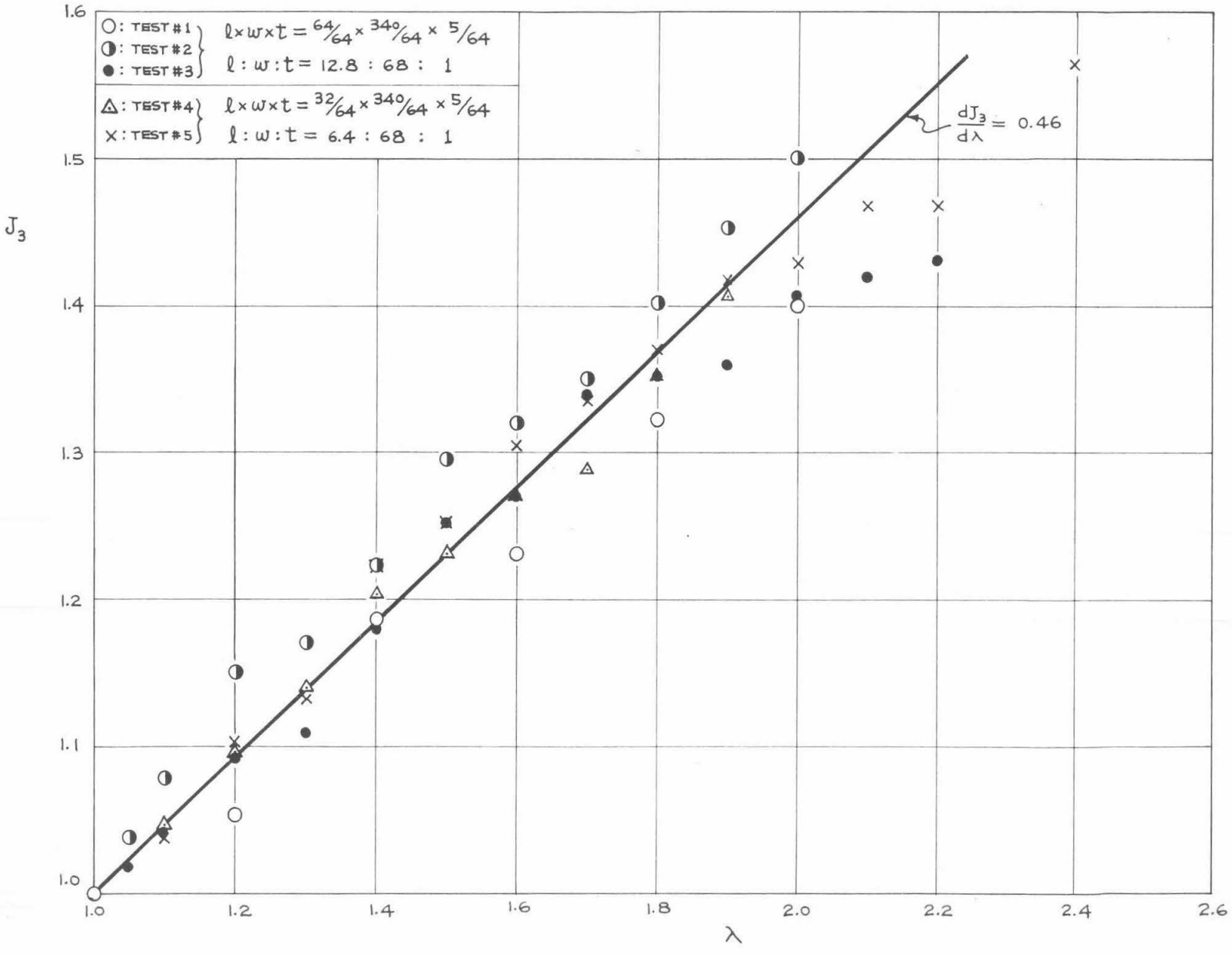

FIG. I. 11. UNIAXIAL STRESS V.S. LONGITUDINAL EXTENSION RATIO (PU-FOAM)

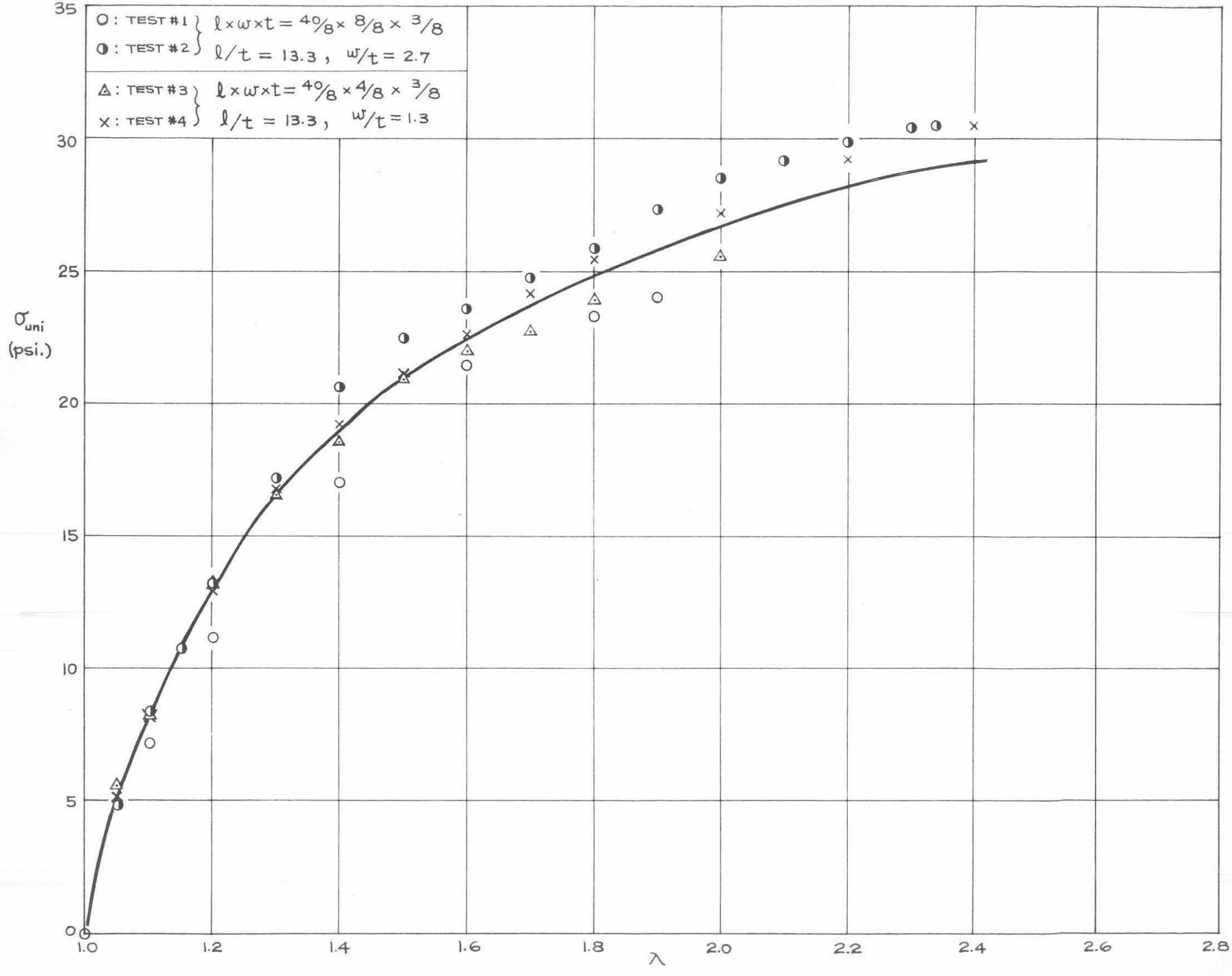

FIG. I.12. EVALUATION OF W_1 & W_2 FROM RECTIFIED UNIAXIAL DATA

PU-FOAM

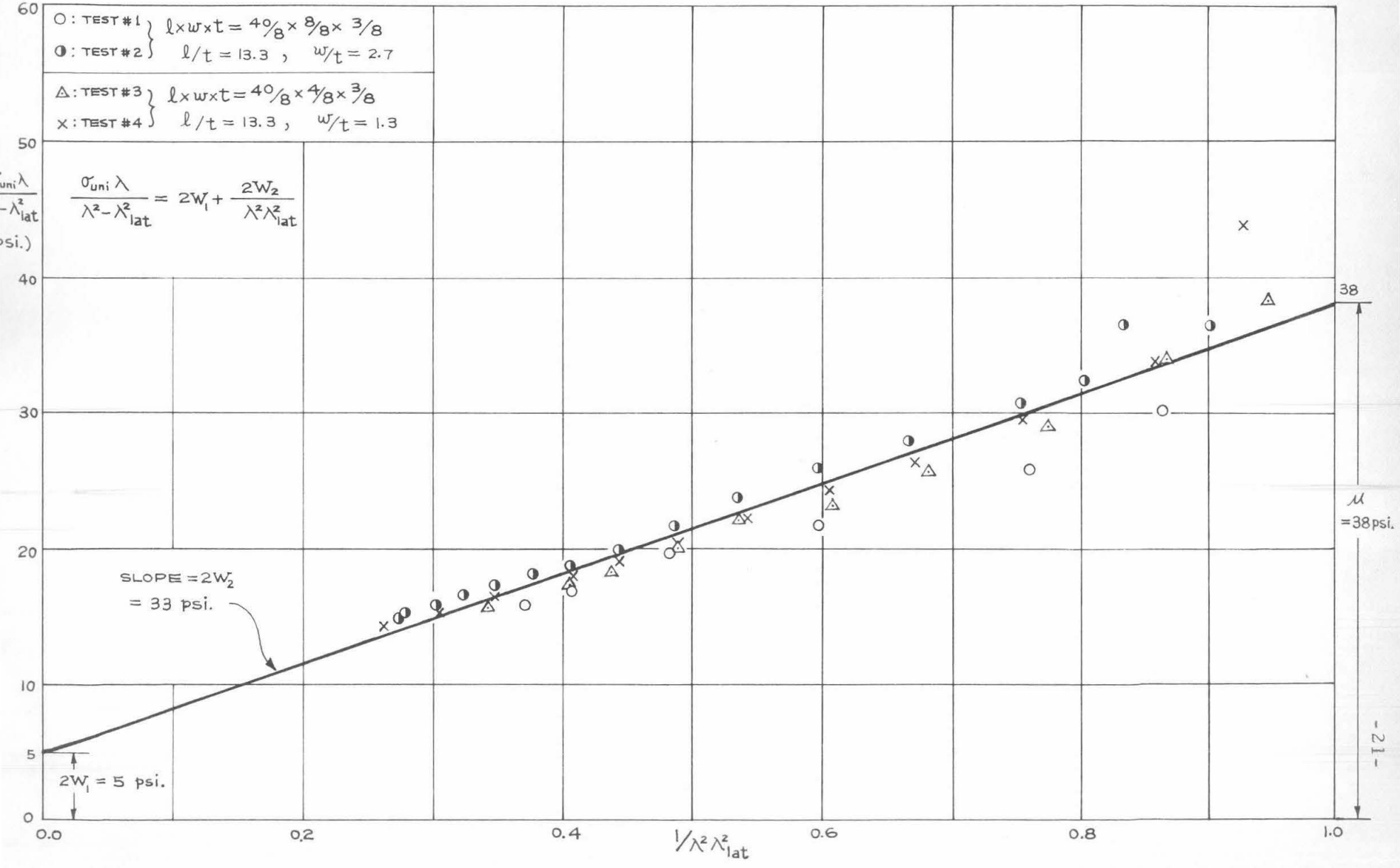

FIG. I. 13. UNIAXIAL LATERAL CONTRACTION RATIO V.S. LONGITUDINAL EXTENSION RATIO

PU - FOAM

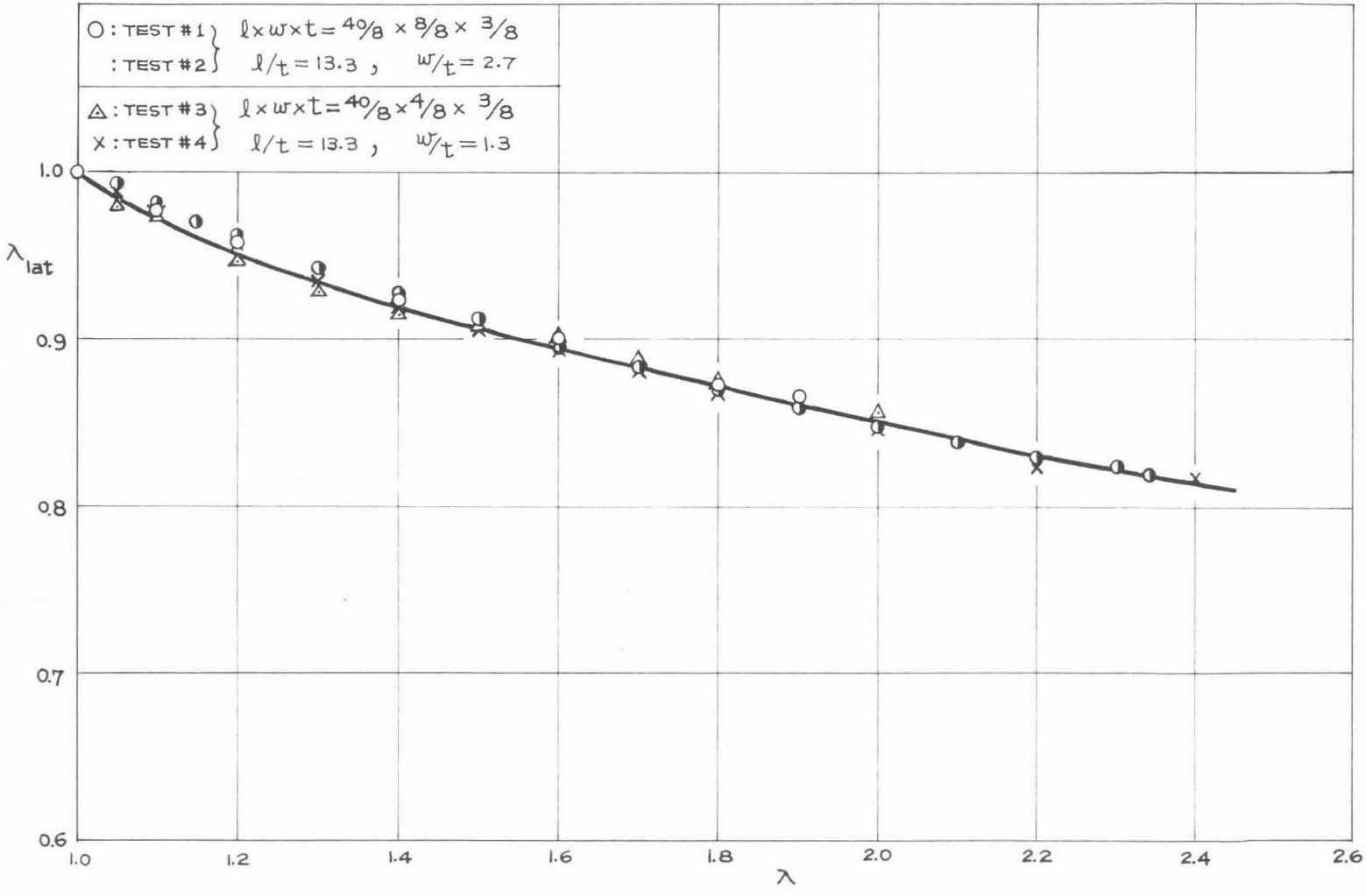

FIG.I.14. UNIAXIAL DILATATION V.S. LONGITUDINAL EXTENTION RATIO

PU – FOAM

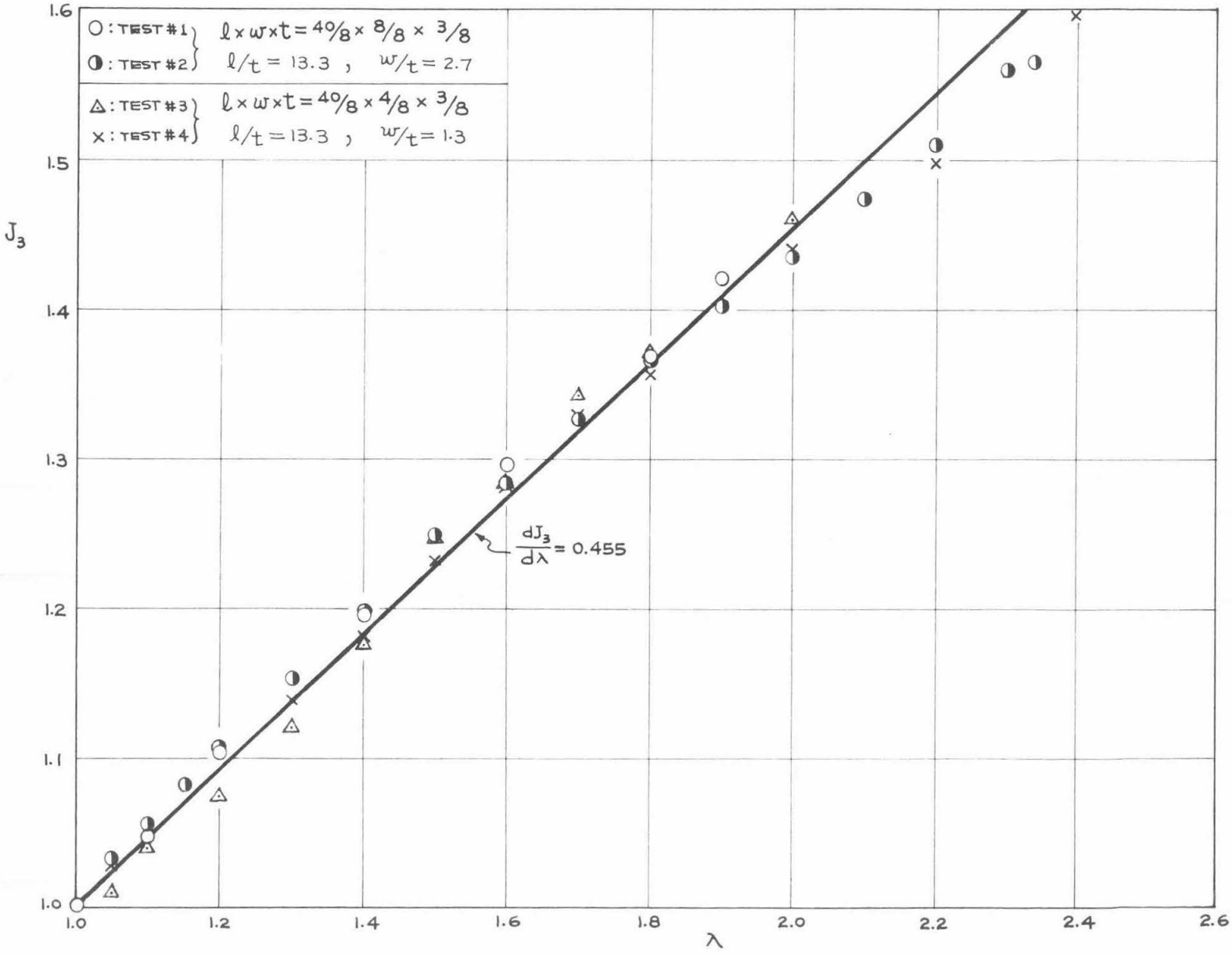

FIG. I. 15. BIAXIAL STRESS VS. LONGITUDINAL EXTENSION RATIO

PU – FOAM

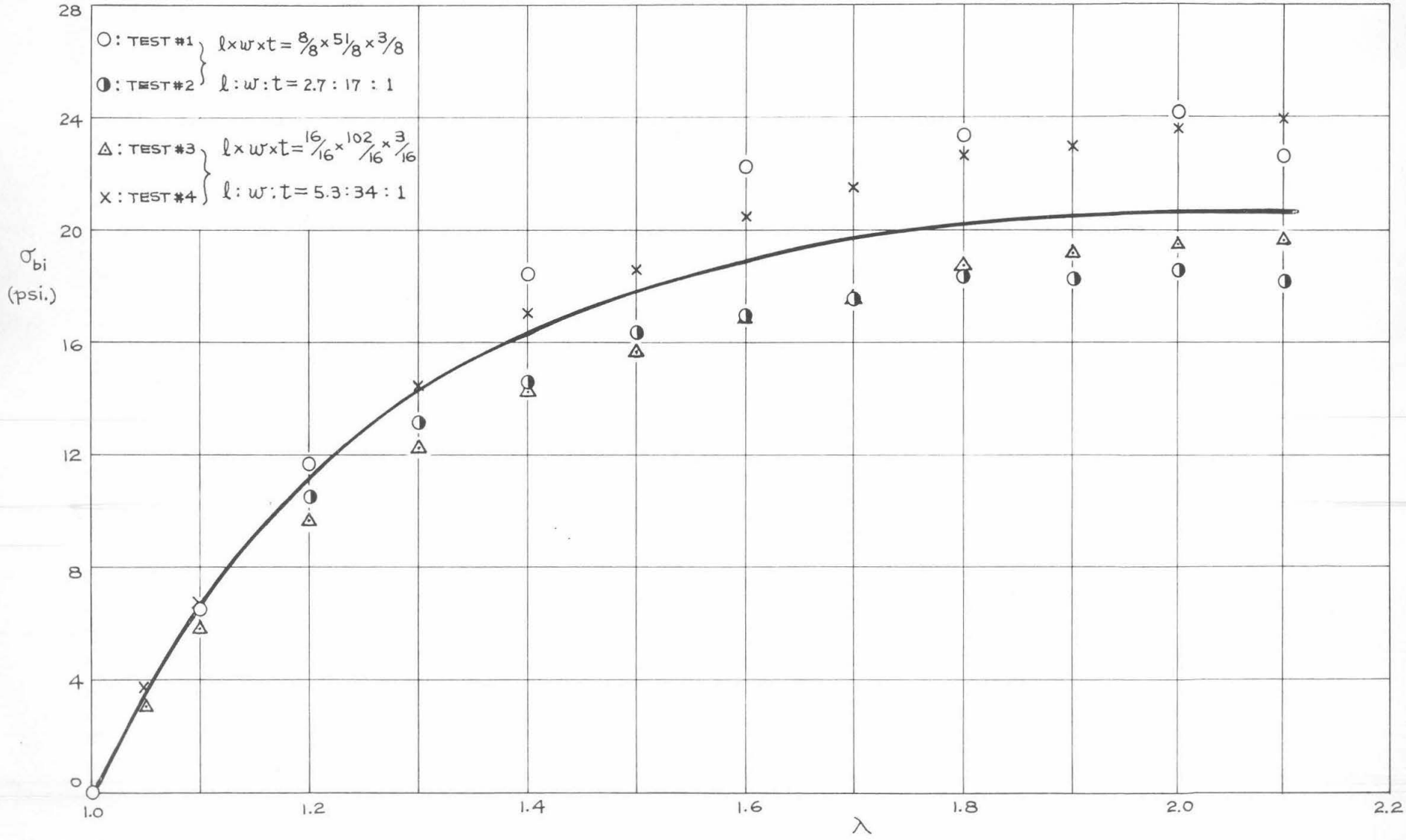

FIG. I.16. EVALUATION OF W_1 & W_2 FROM RECTIFIED BIAXIAL DATA

PU – FOAM

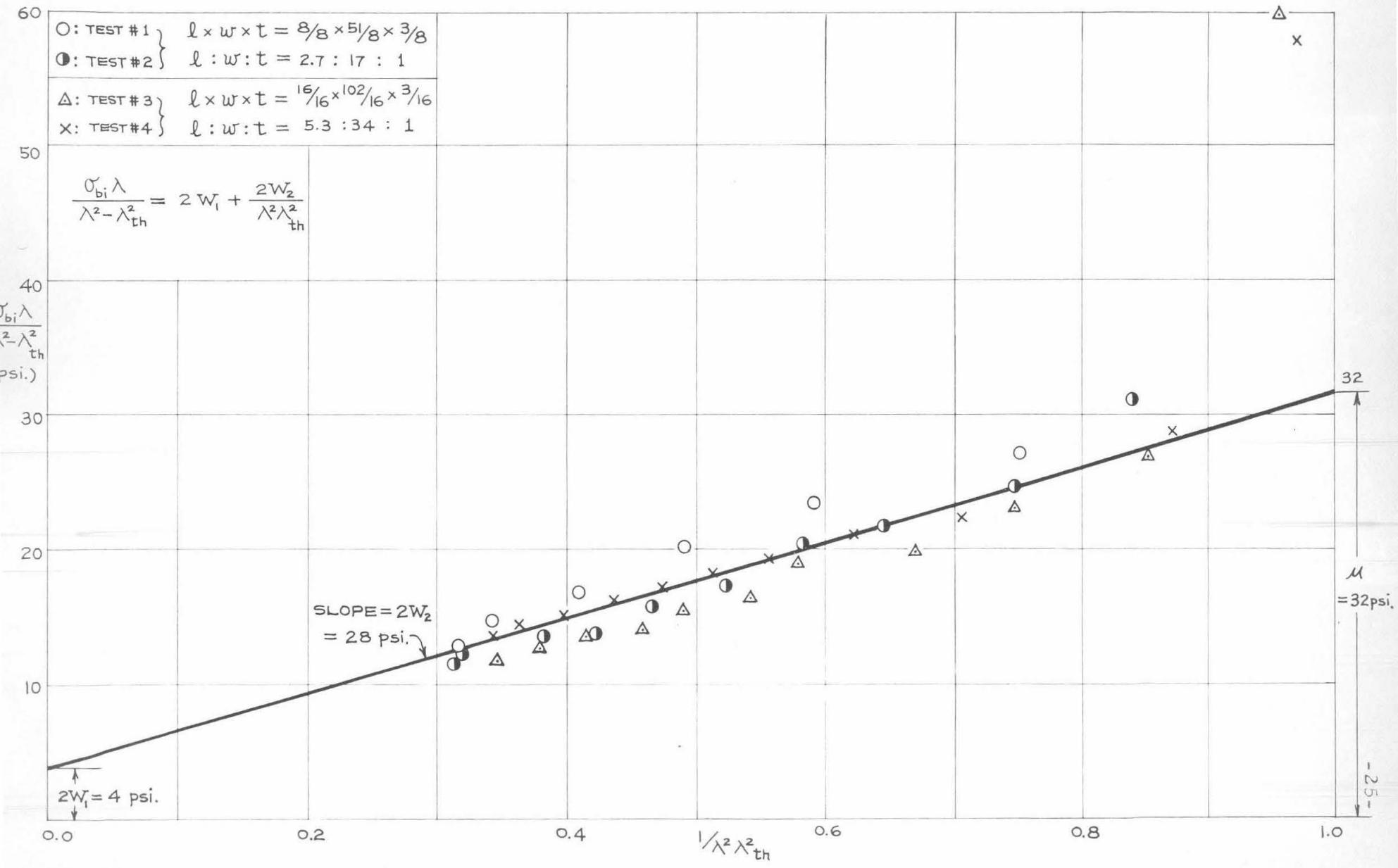

FIG. I. 17. BIAXIAL THICKNESS CONTRACTION RATIO V.S. LONGITUDINAL EXTENSION RATIO

PU-FOAM

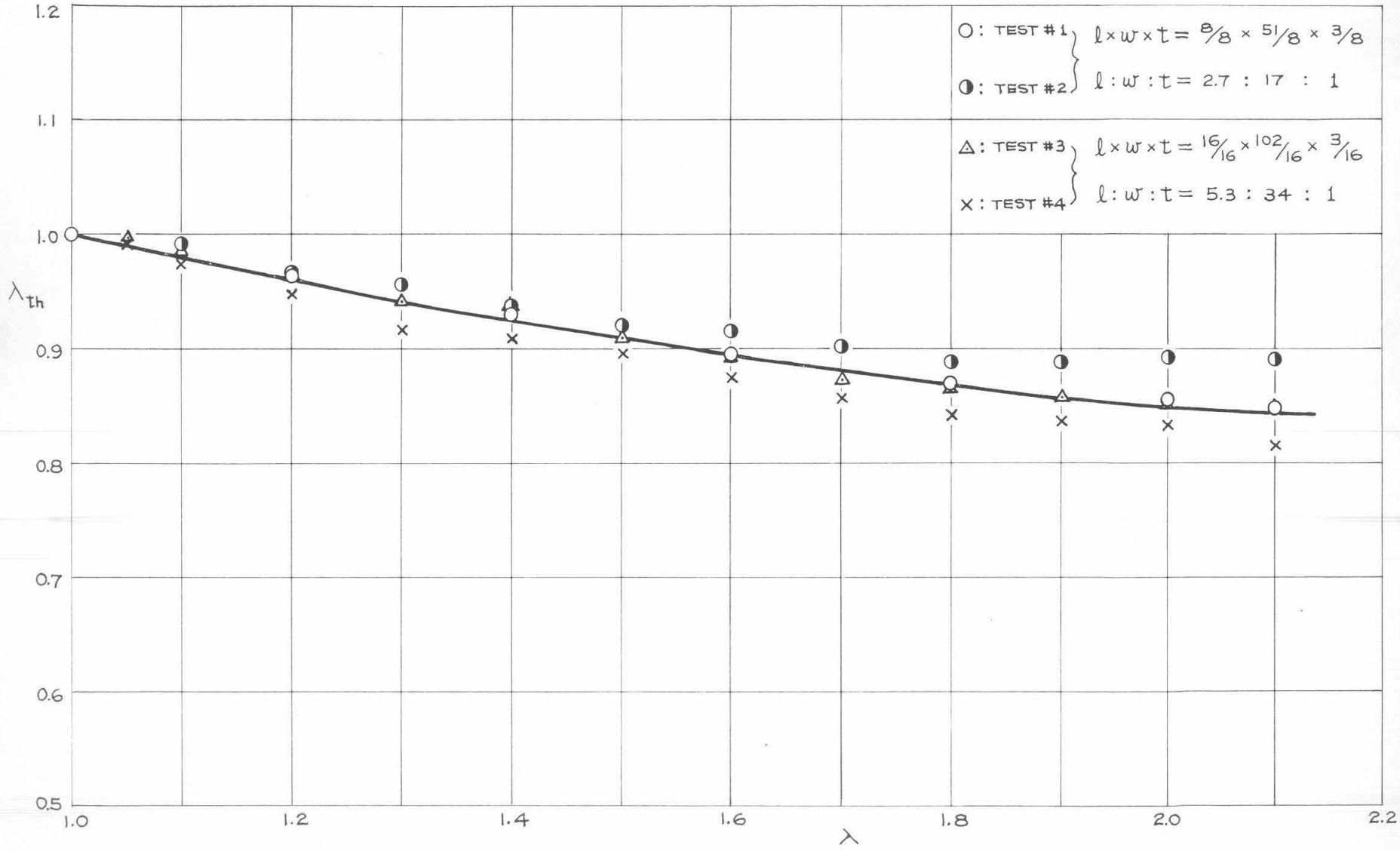

FIG. I.18. BIAXIAL DILATATION V.S. LONGITUDINAL EXTENSION RATIO (PU-FOAM)

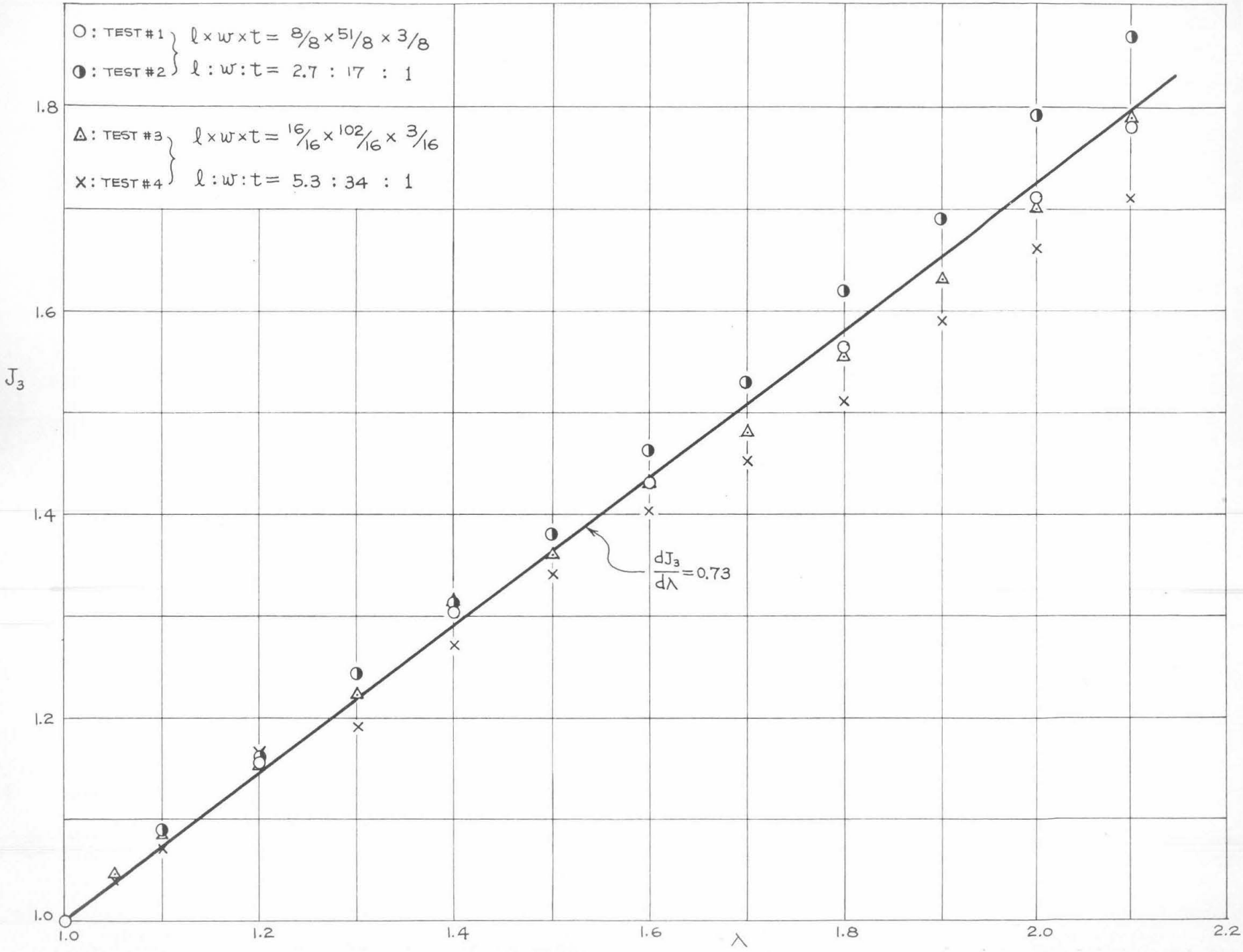

FIG. I. 19. UNIAXIAL STRESS V.S. LONGITUDINAL EXTENSION RATIO [SBR-1500 (3% S)]

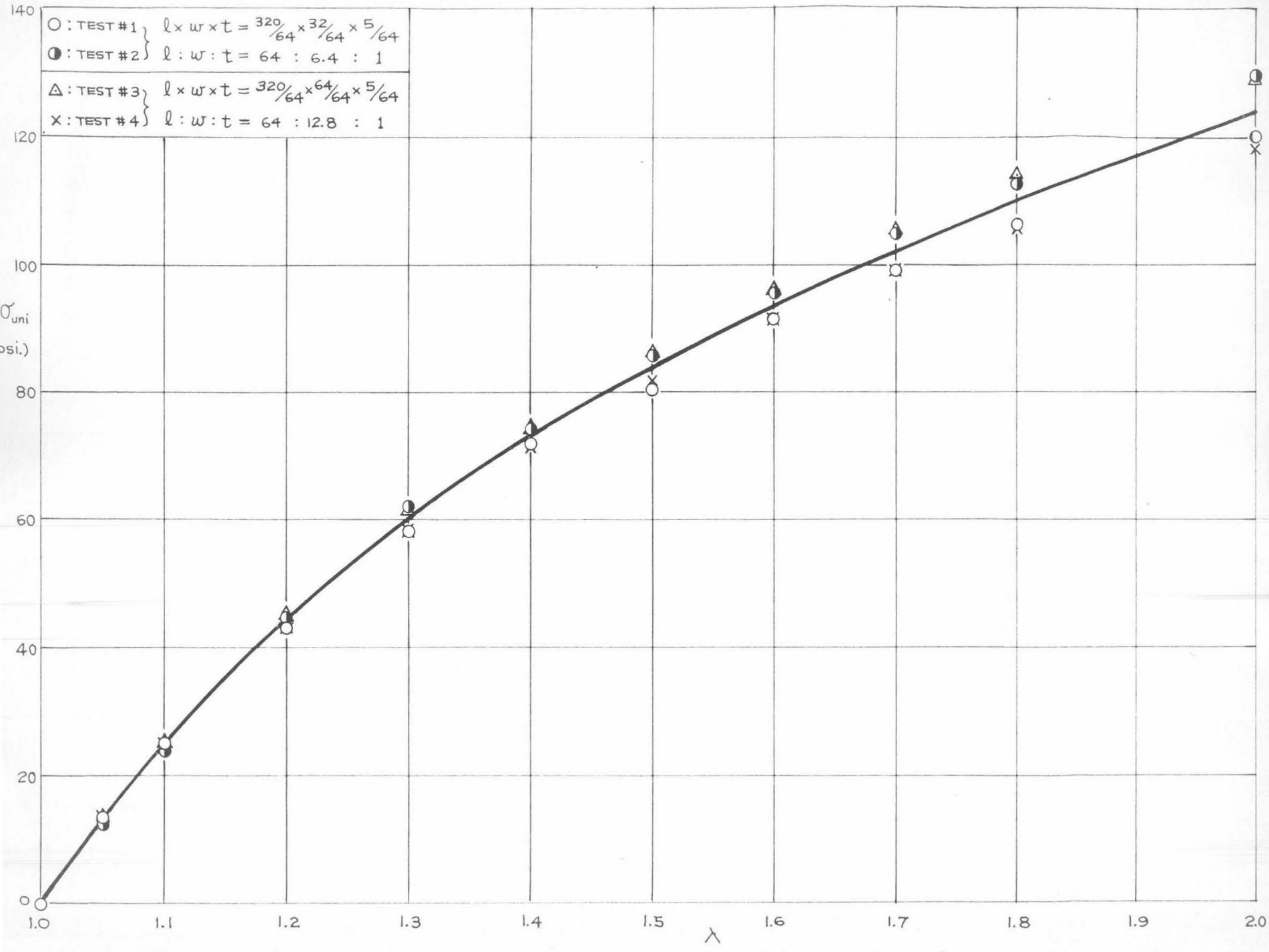

FIG. I.20. EVALUATION OF W_1 & W_2 FROM RECTIFIED UNIAXIAL DATA

SBR-1500 (3% S)

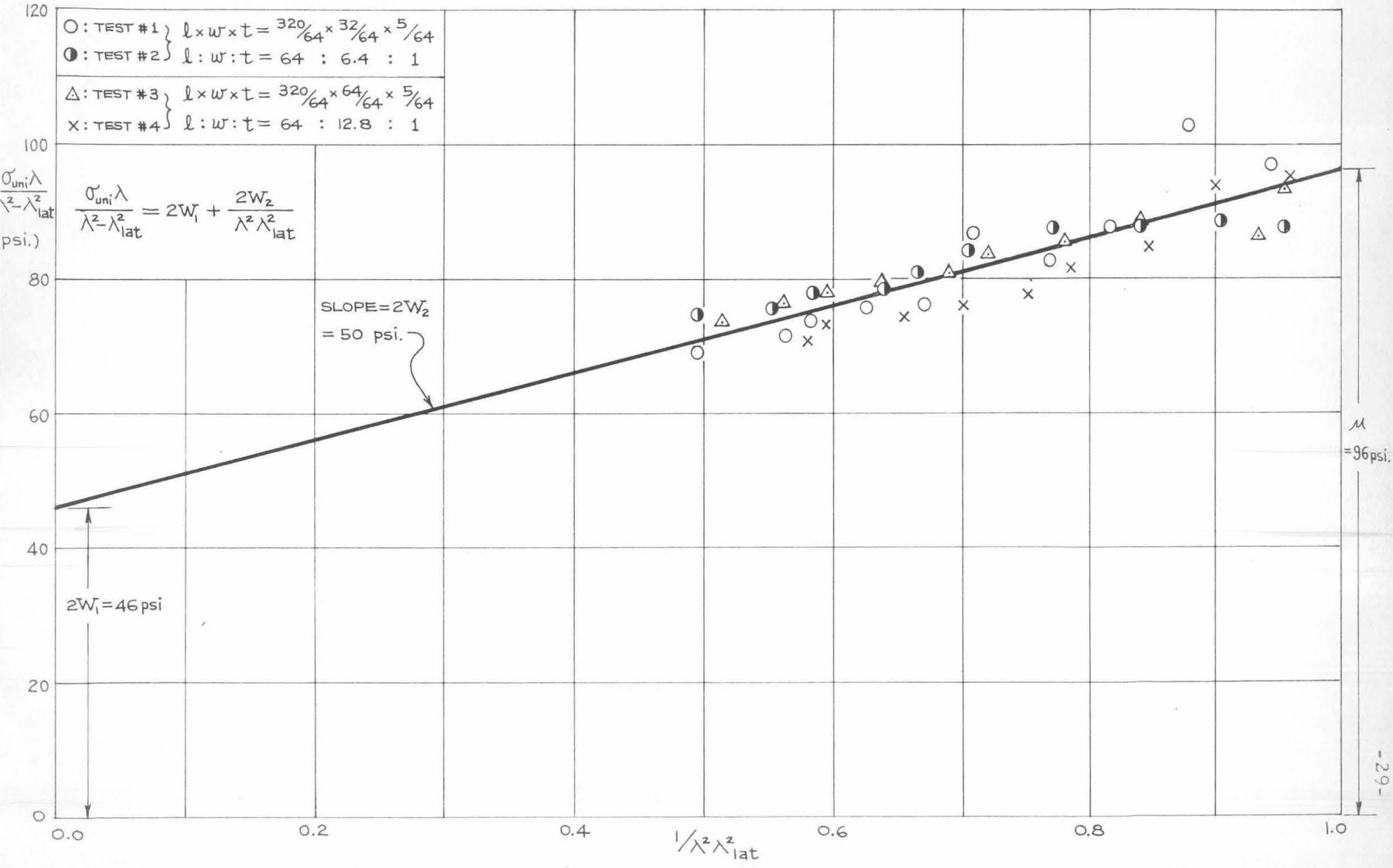

FIG. I. 21. UNIAXIAL LATERAL CONTRACTION RATIO V.S. LONGITUDINAL EXTENSION RATIO

SBR-1500 (3% S)

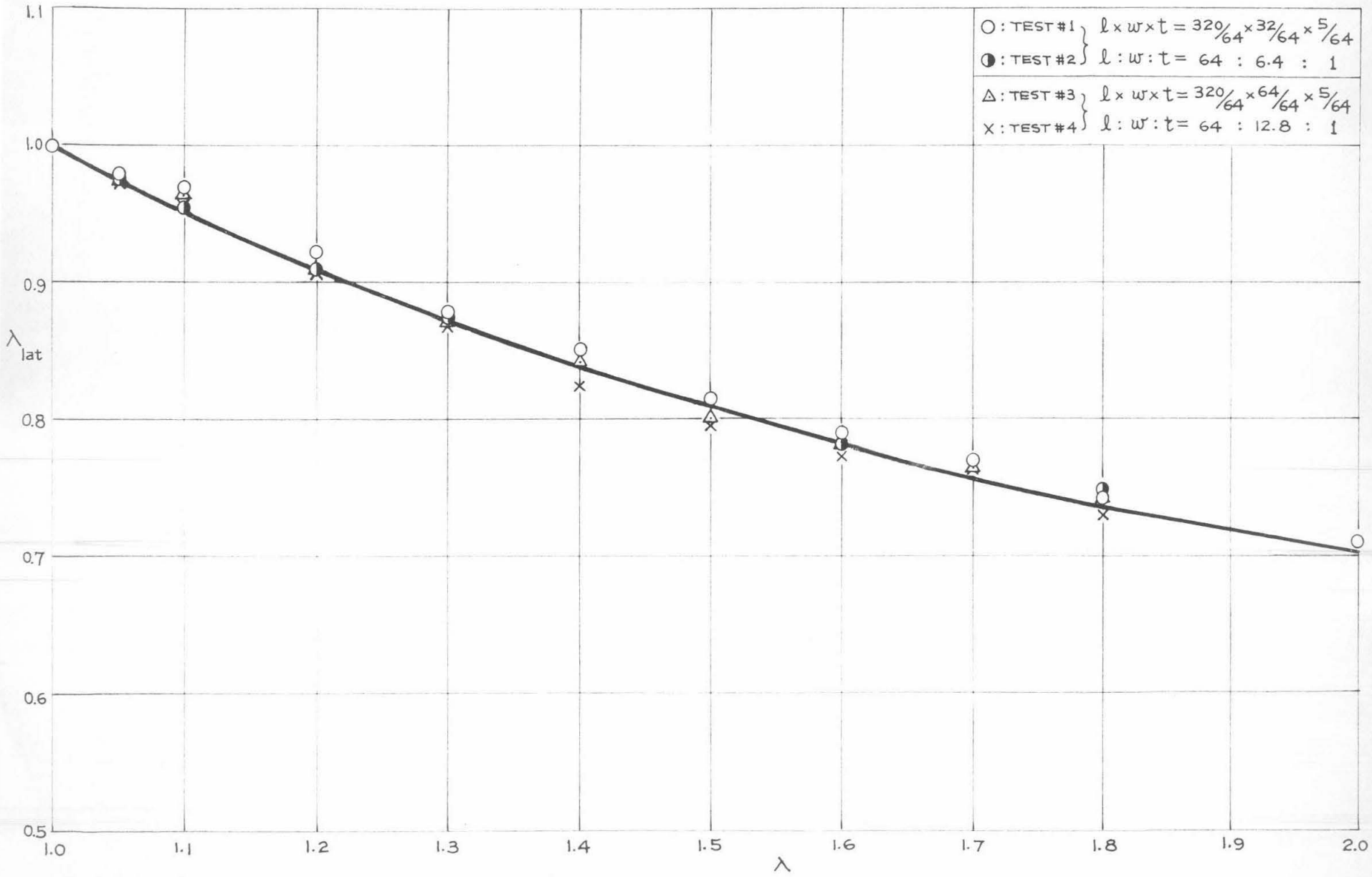

FIG. I. 22. UNIAXIAL DILATATION V.S. LONGITUDINAL EXTENTION RATIO

SBR-1500 (3 % S)

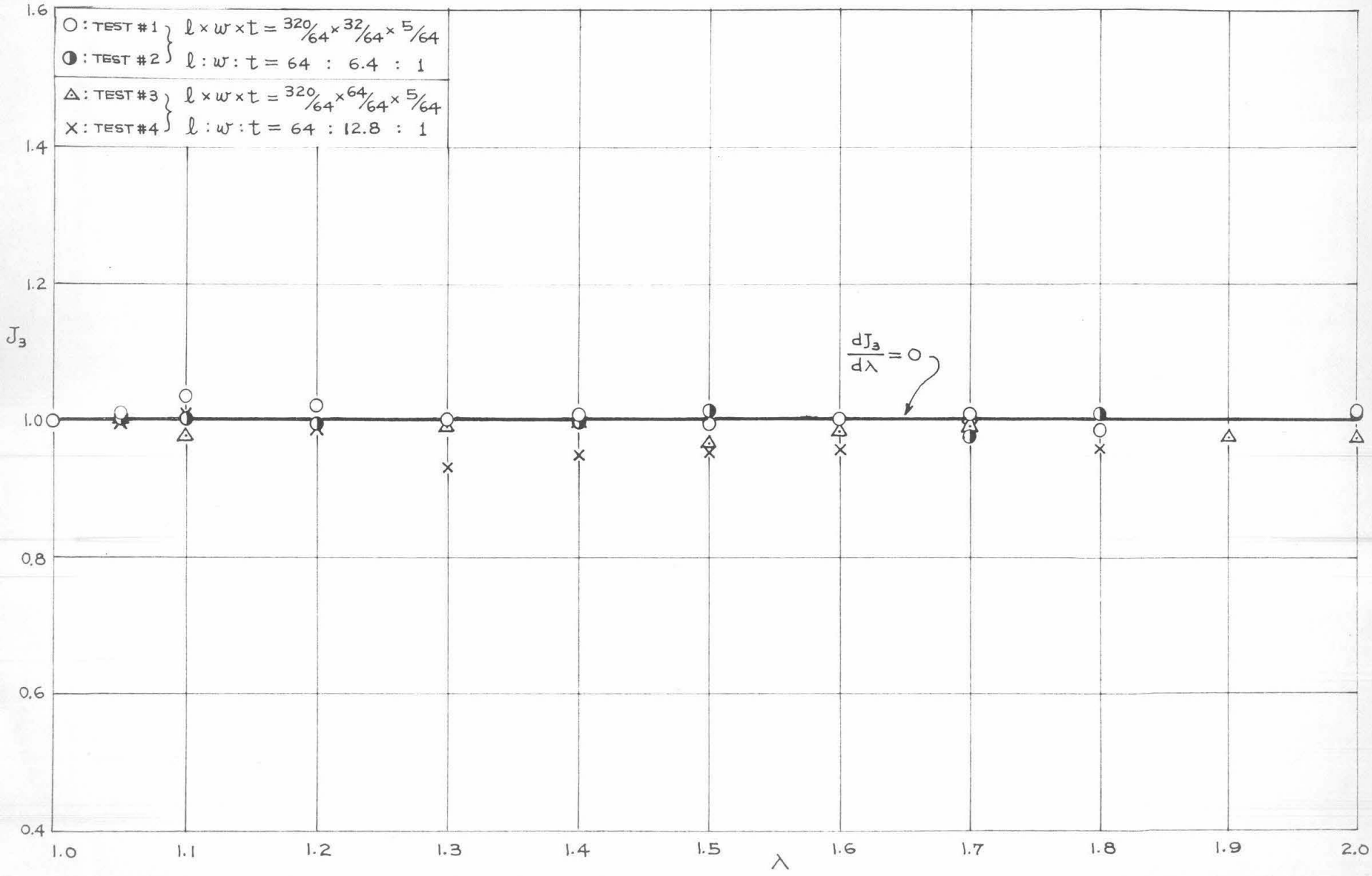

FIG. I. 23. BIAXIAL STRESS V.S. LONGITUDINAL EXTENSION RATIO [SBR-1500(3%S)]

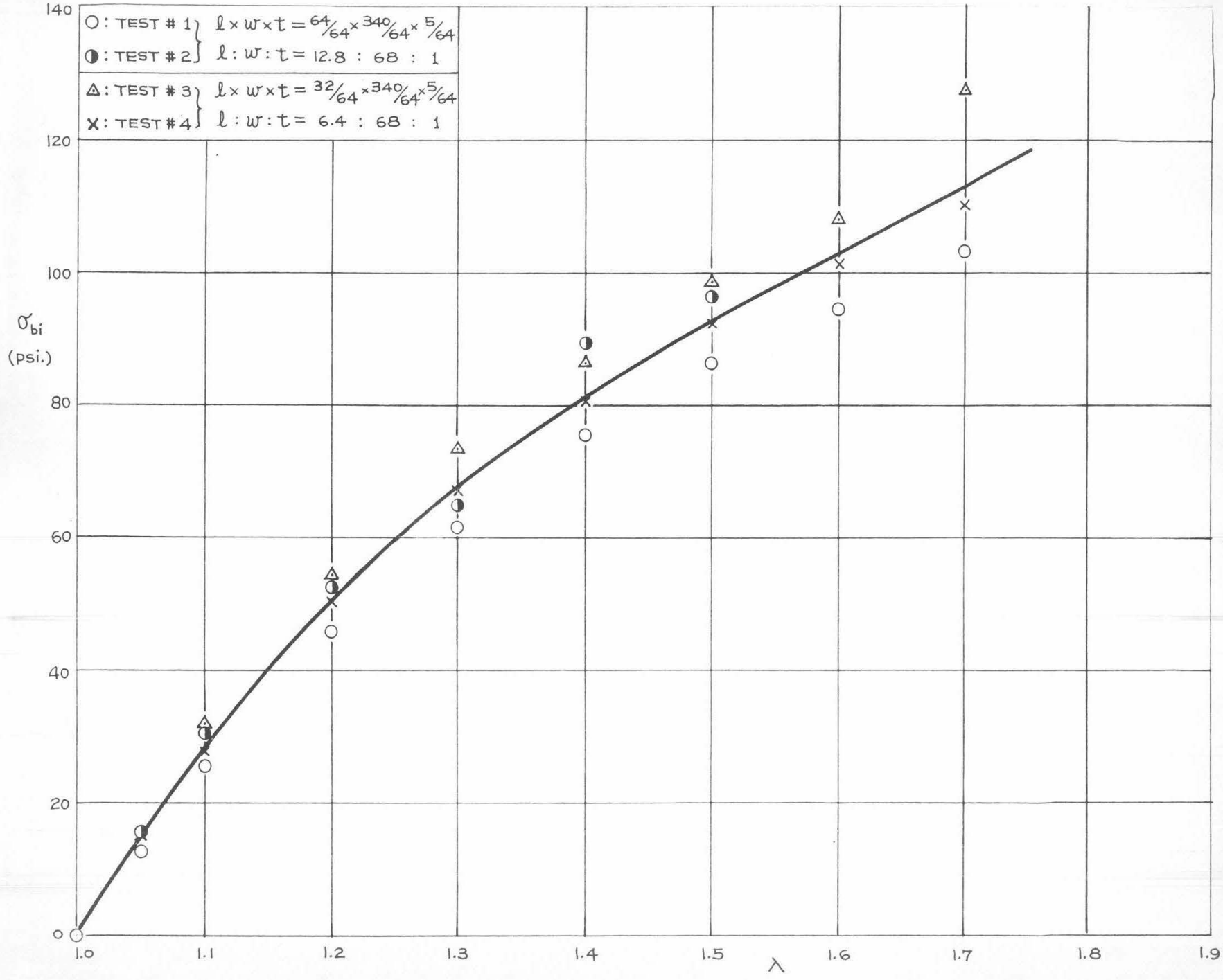

FIG. I.24. EVALUATION OF W_1 & W_2 FROM RECTIFIED BIAXIAL DATA

SBR-1500 (3 % S)

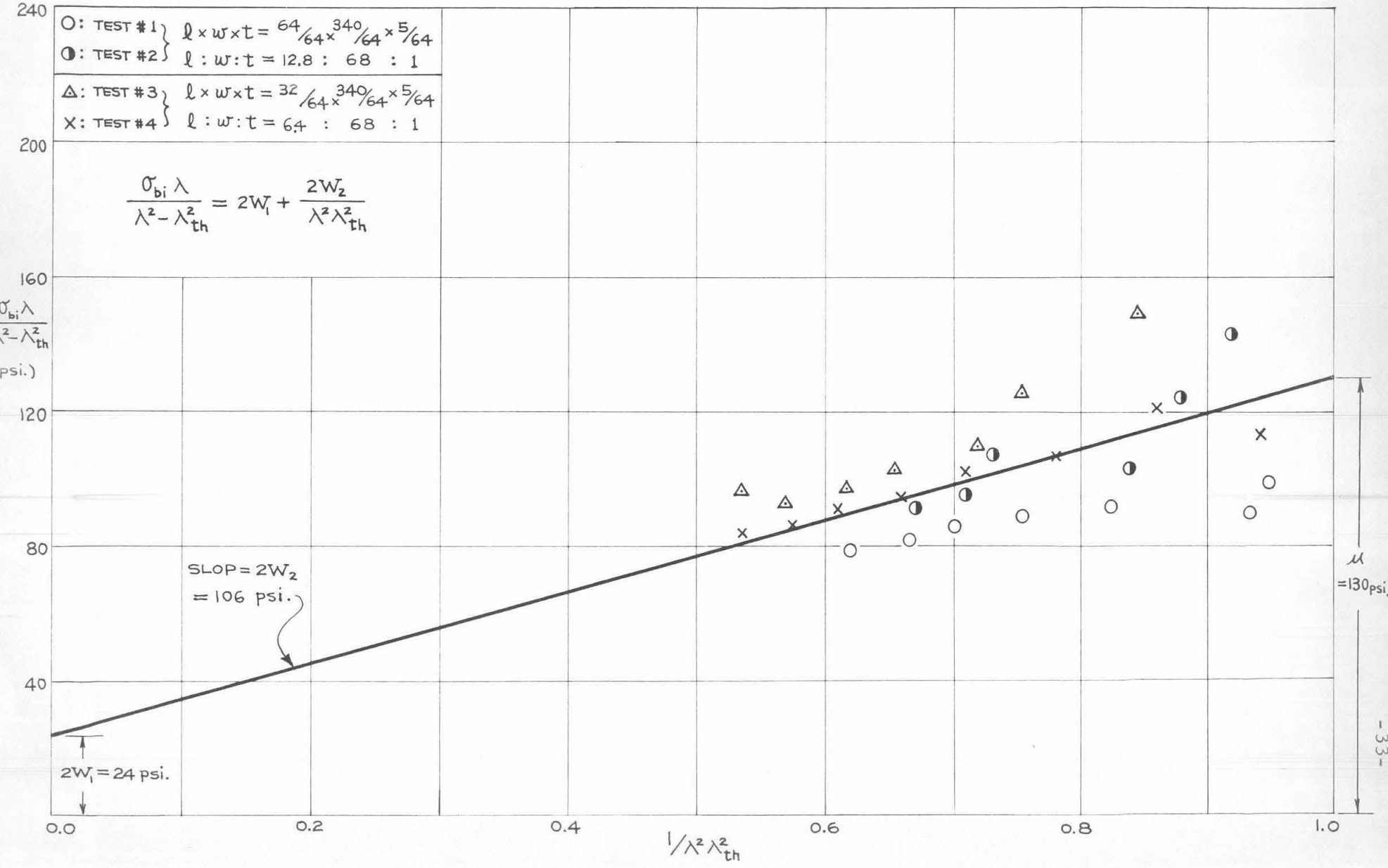

FIG. I. 25 BIAXIAL THICKNESS CONTRACTION RATIO V.S. LONGITUDINAL EXTENSION RATIO

SBR-1500 (3% S)

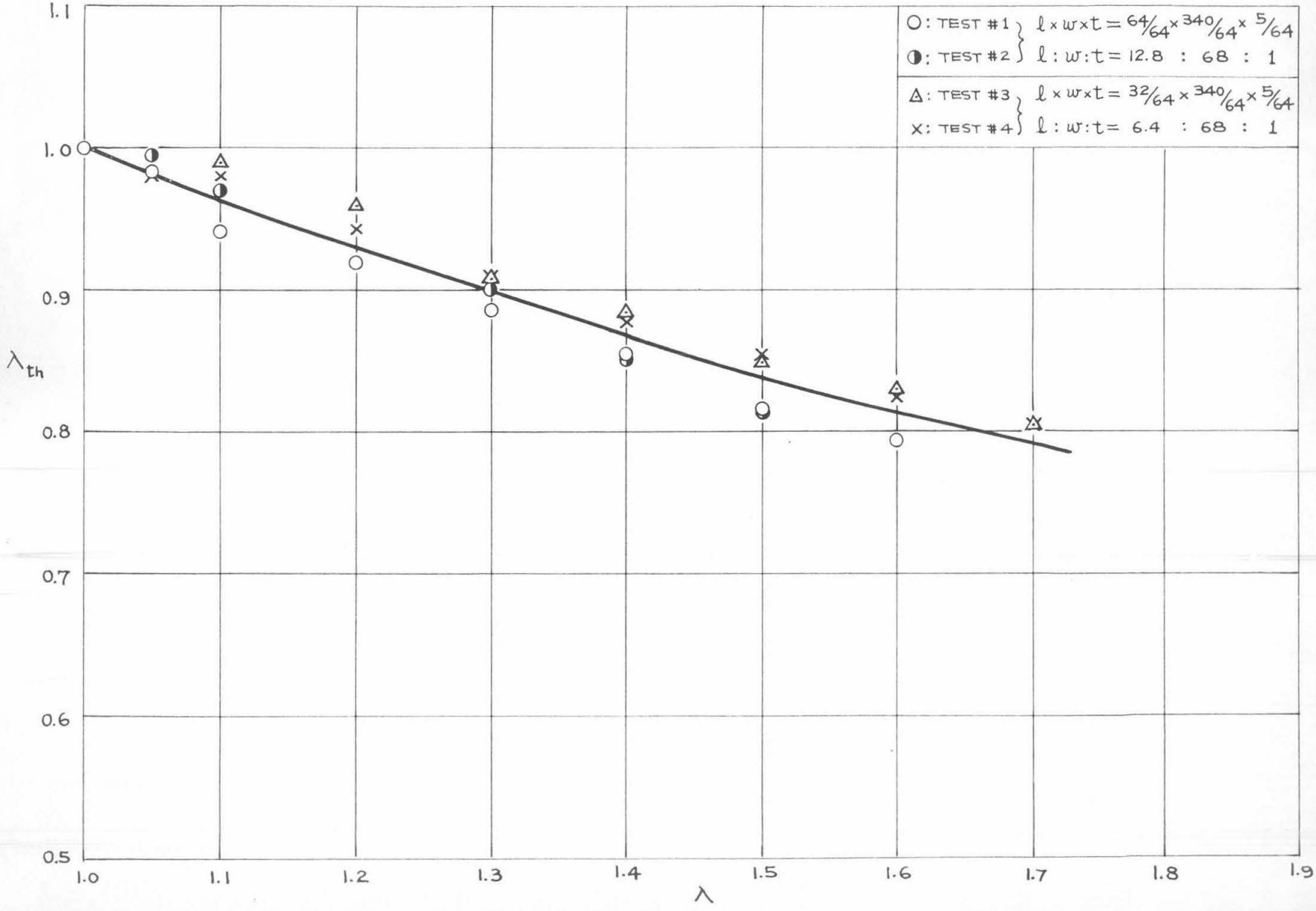

FIG. I. 26. BIAXIAL DILATATION V.S. LONGITUDINAL EXTENSION RATIO

SBR-1500 (3 % S)

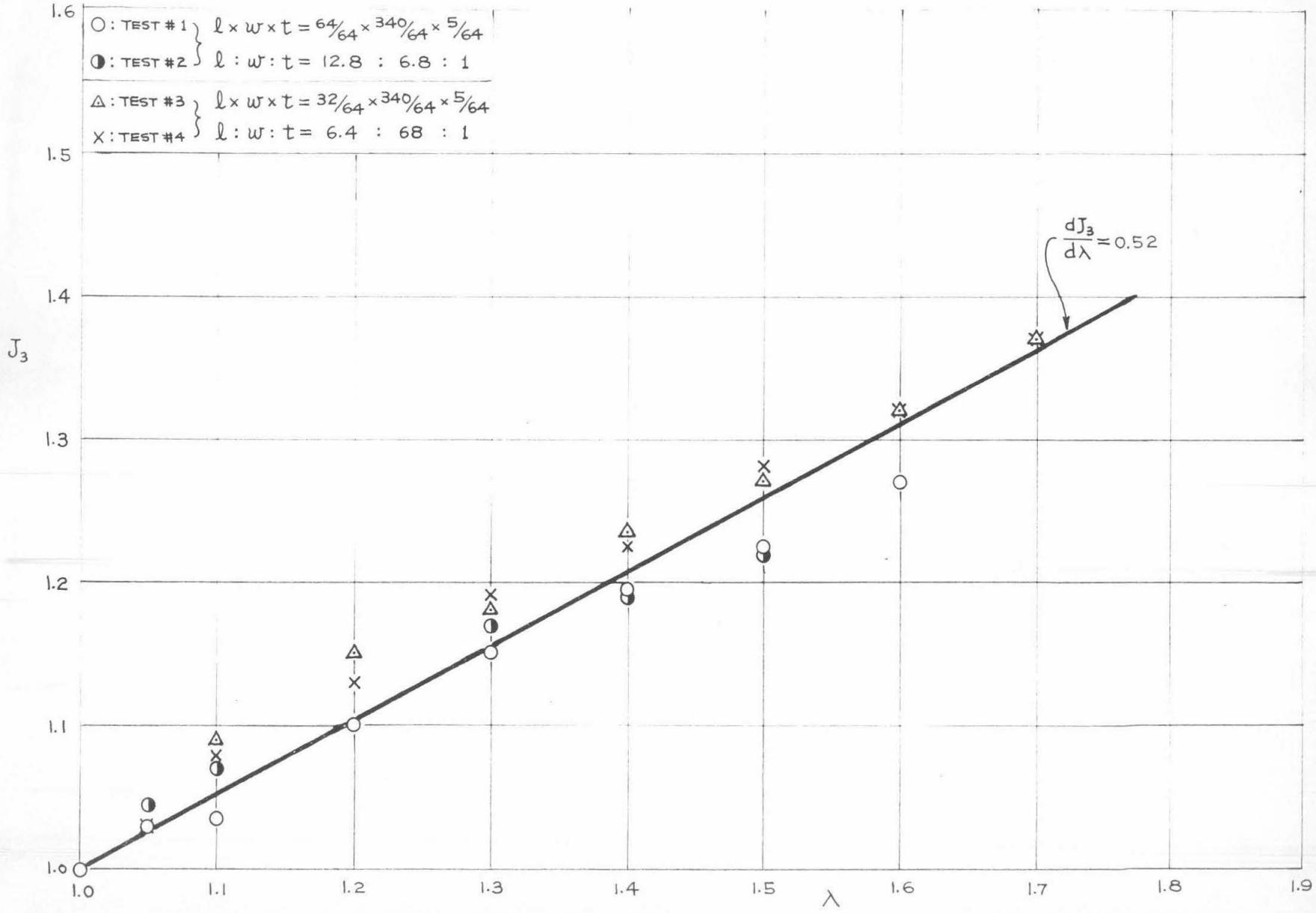

IV. STRESS ANALYSIS

A. Introduction

As a result of elaborate studies of the restrictions imposed upon interior ballistic design by exterior ballistic considerations, most large case-bonded solid propellant rocket motors possess a small aspect ratio, of the order of three to one. This means that the assumptions made in a plane strain analysis generate a solution which is valid only over a very small fraction of the length of the grain. Thus the problem of obtaining useful solutions near the ends of a grain becomes important. In effect this is being done experimentally by photoelastic technique and analytically by the relaxation technique. Unfortunately in both these cases, no estimate of the error involved at the corner is generated. The corner problem entails its own unique analytic features which are incompatible with the behavior of real materials and incompatible with the assumptions of relaxation.

Thus two problems demand attention. In order for the engineer to predict yield or some form of failure due to high stresses at a corner he must first have the elastic stress field for a perfectly elastic material. But in order to obtain this rapidly with the aid of a relaxation technique, he must first solve the particular analytic problem close to the corner. The complexity of this corner problem depends intimately on the geometry of the body. We propose to study this problem in four steps.

First we shall consider the plane strain and plane stress deformation of an elastic sector-space, subjected to the condition of clamped-free boundaries. Secondly, in a subsequent report we shall consider the plane strain and plane stress deformation of an elastic slab. Subsequent treatments will deal with the elastic column subjected to radial tension or compression, free axial face; and lastly subjected to axial tension or compression, free radial face. The last problem refers to the so called parallel-plate test used for determination of the dilatational component of the strain energy.

B. Elastic Field in a Clamped-Free Sector-Space

1. Geometry

For the purpose of this discussion, the elastic sector-space will be bounded by two edges - one free located at $\theta = 0$, and one clamped located at $\theta = \alpha$. In the case $\alpha > \pi$, the sector deficiency of the total space will be termed a crack of flank angle $(2\pi - \alpha)$. And as $\alpha \to 2\pi$, the crack degenerates to a radial line. In the generalized sense, the term space encompasses the two limiting structures of infinite and zero thicknesses. In the former case, the bounderies are planes; in the latter, edges. The language of the associated analysis will be couched in terms of the parameter σ which, for plane strain, is identical with ν, and which, for plane stress, is replaced by $\nu/(1+\nu)$. It is convenient to refer the corner of the space to the origin of a system of polar coordinates; the two edges are then geometrized as rays.

2. The Biharmonic Function

Under the influence of arbitarily imposed surface tractions and displacements (no body forces) equilibrium in the plane elastic field is represented by the solution of the following equations:

$$\frac{\partial \sigma_r}{\partial r} + \frac{\sigma_r - \sigma_\theta}{r} + \frac{1}{r}\frac{\partial \tau_{r\theta}}{\partial \theta} = 0 \qquad \text{(IV. 1)}$$

$$\frac{\partial \tau_{r\theta}}{\partial r} + \frac{2\tau_{r\theta}}{r} + \frac{1}{r}\frac{\partial \sigma_\theta}{\partial \theta} = 0 \qquad \text{(IV. 2)}$$

$$\frac{\partial \sigma_z}{\partial z} = 0 \qquad \text{(IV. 3)}$$

$$\tau_{rz} = \tau_{\theta z} = 0 \qquad \text{(IV. 4)}$$

Application of the method of characteristics to (IV. 1), (IV. 2) introduces the stress function Φ from which the stresses are generated by:

$$\sigma_r = \frac{\Phi_r}{r} + \frac{\Phi_{\theta\theta}}{r^2} \qquad \text{(IV. 5)}$$

$$\sigma_\theta = \Phi_{rr} \qquad \text{(IV. 6)}$$

$$\tau_{r\theta} = \frac{\Phi_\theta}{r^2} - \frac{\Phi_{r\theta}}{r} \qquad \text{(IV. 7)}$$

The subscripts affixed to Φ denote the appropriate partial differentiation. From Hooke's Law, we have:

$$2\mu\epsilon_r = (1-\sigma)\sigma_r - \sigma\sigma_\theta \qquad \text{(IV. 8)}$$

$$2\mu\epsilon_\theta = (1-\sigma)\sigma_\theta - \sigma\sigma_r \qquad \text{(IV. 9)}$$

$$2\mu\epsilon_z = \sigma_z - \sigma(\sigma_r + \sigma_\theta) = 0 \qquad \text{in plane strain} \qquad \text{(IV. 10a)}$$

$$2\mu\epsilon_z = -\sigma(\sigma_r + \sigma_\theta) \qquad \text{in plane stress} \qquad \text{(IV. 10b)}$$

$$2\mu\epsilon_{r\theta} = \tau_{r\theta} \qquad \text{(IV. 11)}$$

$$\epsilon_{rz} = \epsilon_{\theta z} = 0 \qquad \text{(IV. 12)}$$

The strains are generated from three displacement components

u for radial

v for tangential

w for axial, as follows:

$$\epsilon_r = \frac{\partial u}{\partial r} \tag{IV. 13}$$

$$\epsilon_\theta = \frac{u}{r} + \frac{1}{r}\frac{\partial v}{\partial \theta} \tag{IV. 14}$$

$$\epsilon_{r\theta} = \frac{1}{2}\left(\frac{1}{r}\frac{\partial u}{\partial \theta} + \frac{\partial v}{\partial r} - \frac{v}{r}\right) \tag{IV. 15}$$

$$\epsilon_z = \frac{\partial w}{\partial z} = 0, \qquad w = 0 \quad \text{, for plane strain} \tag{IV. 16a}$$

$$\frac{\partial w}{\partial z} = \text{harmonic function , for plane stress} \tag{IV. 16b}$$

Since ϵ_r, ϵ_θ, and $\epsilon_{r\theta}$ are generated from only two of the three displacement components, their compatibility with simply-connected Eucledean space must be guaranteed. Elimination of u and v from (IV. 13), (IV. 14), (IV. 15) yields

$$2\left(\frac{1}{r}\epsilon_{r\theta,r\theta} + \frac{1}{r^2}\epsilon_{r\theta,\theta}\right) = \epsilon_{\theta,rr} + \frac{2}{r}\epsilon_{\theta,r} + \frac{1}{r^2}\epsilon_{r,\theta\theta} - \frac{1}{r}\epsilon_{r,r} \tag{IV. 17}$$

Returning to (IV. 5), (IV. 6), (IV. 7), via (IV. 8), (IV. 9), we find that the compatibility of the strain components specifies the character of Φ :

$$\Phi_{rrrr} + \frac{2}{r}\Phi_{rrr} - \frac{1}{r^2}\Phi_{rr} + \frac{1}{r^3}\Phi_r + \frac{2}{r^2}\Phi_{rr\theta\theta} - \frac{2}{r^3}\Phi_{r\theta\theta} + \frac{4}{r^4}\Phi_{\theta\theta} + \frac{1}{r^4}\Phi_{\theta\theta\theta\theta} = 0 \tag{IV. 18a}$$

or
$$\left(\frac{\partial^2}{\partial r^2} + \frac{1}{r}\frac{\partial}{\partial r} + \frac{1}{r^2}\frac{\partial^2}{\partial \theta^2}\right)^2 \Phi \equiv \nabla^4 \Phi = 0 \tag{IV. 18b}$$

Equation (IV. 18b) is termed polar biharmonic because it expresses the iterated application of the polar Laplacian on the stress function. Because of the degeneracy of the roots of the characteristic equation, representing (IV. 18b), care must be exercised in expressing the complete

set of solutions which span the biharmonic field. Noting first that (IV. 18a) is differentially homogeneous in r^4, we set $r = e^s$, and write:

$$\Phi_{ssss} - 4\Phi_{sss} + 4\Phi_{ss} + 2\Phi_{ss\theta\theta} - 4\Phi_{s\theta\theta} + 4\Phi_{\theta\theta} + \Phi_{\theta\theta\theta\theta} = 0 \qquad \text{(IV. 19)}$$

Separation of variables is accomplished by writing $\Phi = S(s) \cdot \Theta(\theta)$, so that:

$$S'''' - 4S''' + S''\left(4 + 2\frac{\Theta''}{\Theta}\right) - 4S'\left(\frac{\Theta''}{\Theta}\right) + S\left(4\frac{\Theta''}{\Theta} + \frac{\Theta''''}{\Theta}\right) = 0 \qquad \text{(IV. 20)}$$

Equation (IV. 20) is the characteristic representation of (IV. 18a) and is meaningful only for the substitutions:

$$\frac{\Theta''}{\Theta} = 0,\ \pm k^2,\ \frac{2}{\theta \tan\theta} - 1\ ,\ \frac{2\tan\theta}{\theta} - 1$$

Let us consider each of five substitutions in turn:

a) $\Theta'' = 0$, $\Theta = A + B\theta$.

$$S'''' - 4S''' + 4S'' = 0 \qquad \text{(IV. 21)}$$

$$D^4 - 4D^3 + 4D^2 \equiv D^2(D-2)^2 = 0 \qquad \text{(IV. 22)}$$

$$S = C + Ds + Ee^{2s} + Fse^{2s} \qquad \text{(IV. 23)}$$

$$\Phi = (A + B\theta)(C + D\ln r + Er^2 + Fr^2 \ln r) \qquad \text{(IV. 24)}$$

b) $\Theta'' = k^2\Theta$, $\Theta = A\sinh k\theta + B\cosh k\theta$

$$S'''' - 4S''' + S''(4 + 2k^2) - 4k^2S' + S(4k^2 + k^4) = 0 \qquad \text{(IV. 25)}$$

$$D^4 - 4D^3 + 2(2+k^2)D^2 - 4k^2 D + k^2(k^2+4)$$
$$\equiv (D+ik)(D-ik)(D-2+ik)(D-2-ik) = 0 \qquad \text{(IV. 26)}$$

$$S = C\sin ks + D\cos ks + Fe^{2s}\sin ks + Fe^{ks}\cos ks \qquad \text{(IV. 27)}$$

$$\Phi = (A\sinh k\theta + B\cosh k\theta)(C\sin k\ln r + D\cos k\ln r + Er^2\sin k\ln r + Fr^2\cos k\ln r) \qquad \text{(IV. 28)}$$

c) $\Theta'' = -k^2\Theta$, $\Theta = A\sin k\theta + B\cos k\theta$

$$S'''' - 4S''' + S''(4-2k^2) + 4k^2 S' + S(k^4 - 4k^2) = 0 \qquad \text{(IV. 29)}$$

$$D^4 - 4D^3 + 2(2-k^2)D^2 + 4k^2 D + k^4 - 4k^2$$
$$\equiv (D+k)(D-k)(D-2+k)(D-2-k) = 0 \qquad \text{(IV. 30)}$$

$$S = C\sinh ks + D\cosh ks + Ee^{2s}\sinh ks + Fe^{2s}\cosh ks \qquad \text{(IV. 31)}$$

$$\Phi = (A\sin k\theta + B\cos k\theta)(Ce^{k\ln r} + De^{-k\ln r} + Er^2 e^{k\ln r} + Fr^2 e^{-k\ln r}) \qquad \text{(IV. 32a)}$$

$$\Phi = (A\sin k\theta + B\cos k\theta)(Cr^k + Dr^{-k} + Er^{2+k} + Fr^{2-k}) \qquad \text{(IV. 32b)}$$

d) $\Theta'' = \Theta\left(\frac{2}{\theta\tan\theta} - 1\right)$, $\Theta = \theta\sin\theta$

$$S'''' - 4S''' + S''\left(2 + \frac{4}{\theta\tan\theta}\right) - 4S'\left(\frac{2}{\theta\tan\theta} - 1\right) + S\left(\frac{4}{\theta\tan\theta} - 3\right) = 0 \qquad \text{(IV. 33)}$$

$$S'''' - 4S''' + 2S'' + 4S' - 3S \equiv (D-1)^2(D+1)(D-3) = 0 \qquad \text{(IV. 34a)}$$

$$4S'' - 8S' + 4S \equiv (D-1)^2 = 0 \qquad \text{(IV. 34b)}$$

$$S = Ae^s + Bse^s \qquad \text{(IV. 35)}$$

$$\Phi = \theta \sin\theta\,(Ar + Br\ln r) \qquad \text{(IV. 36)}$$

e) $$\Theta'' = -\Theta\left(1 + \frac{2\tan\theta}{\theta}\right), \qquad \Theta = \theta\cos\theta$$

$$S'''' - 4S''' + S''\left(2 - \frac{4\tan\theta}{\theta}\right) + 4S'\left(1 + \frac{2\tan\theta}{\theta}\right) - S\left(3 + \frac{4\tan\theta}{\theta}\right) = 0 \qquad \text{(IV. 37)}$$

$$S'''' - 4S''' + 2S'' + 4S' - 3S \equiv (D-1)^2(D+1)(D-3) = 0 \qquad \text{(IV. 38a)}$$

$$-4S'' + 8S' - 4S \equiv -(D-1)^2 = 0 \qquad \text{(IV. 38b)}$$

$$S = Ae^s + Bse^s \qquad \text{(IV. 39)}$$

$$\Phi = \theta\cos\theta\,(Ar + Br\ln r) \qquad \text{(IV. 40)}$$

Equations (IV. 21) - (IV. 40) represent the complete set of known analytic solutions to the polar biharmonic. In addition to these, there are presumably a large class of non-analytic functions which represent the application of a biharmonic field to a singular geometry. A complete analysis of these singular fields has not been carried out.

Roughly speaking, solutions of the form (IV. 28) are used when it is desired to expand arbitrary boundary conditions along the boundary rays. In doing this, care must be exercised in approaching the limit $r = 0$; which means in the problem at hand that a small sector of radius ϵ must be cut out of the corner and then be allowed to shrink to zero. By the same token, solutions of the form (IV. 32b) are used when expanding boundary conditions along tangential trajectories, such as when the sector-space is replaced by a finite sector of radius R. In this case care must be exercised in approaching the limits $\theta = 0$ and $\theta = \alpha$. For the most general type of problem - a segment of sector-space bounded by rays $\theta = 0$ and $\theta = \alpha$ and by arcs $r = \epsilon$ and $r = R$, it is necessary to compound linearly solutions of the form (IV. 28) and (IV. 32b) in order to expand arbitrary boundary conditions on all four edges. This becomes quite complicated and tedious. Very often the Fourier sums converge extremely slowly. A great deal of fundamental analysis remains to be done in this problem area.

3. The eigenvalue approach

It is convenient to regroup the terms of (IV. 32b) in order to factor out a single term in r, as follows:

$$\Phi = r^{n+1}\left[A\sin(n+1)\theta + B\cos(n+1)\theta + C\sin(n-1)\theta + D\cos(n-1)\theta\right] \qquad \text{(IV. 41a)}$$

Since it will be shown later on that $|n|< 1$, for the problem at hand, we shall rewrite (IV. 41a) as:

$$\Phi = r^{1+n}\left[A\sin(1+n)\theta + B\cos(1+n)\theta + C\sin(1-n)\theta + D\cos(1-n)\theta\right] \qquad \text{(IV. 41b)}$$

Note that n may be positive or negative. In the latter case, the pre-exponential factor becomes r^{1-n} while the post-trigonometric factor retains its character. The importance of this statement will become apparent.

Since in the problem of sector-space bounded by two rays, only four homogeneous boundary conditions are involved, only four constants A, B, C, D, are needed, and it will be assumed that the space can be spanned by a single eigenvalue. The legitimacy of this assumption remains to be established. In a finite bounded space, at least six or eight boundary conditions are involved, whether homogeneous or not, and in this case n is construed to represent a set of eigenvalues. Furthermore, it is usually necessary to determine two sets of eigenvalues for both radial and tangential expansions. Thus we can attempt to get by with a single eigenvalue only because a sector-space is involved.

4. Eigenvalue solution for a clamped-free quarter space

Sketch 1 reveals the analytic nature of the boundary conditions at the free and clamped edges of a quarter-space.

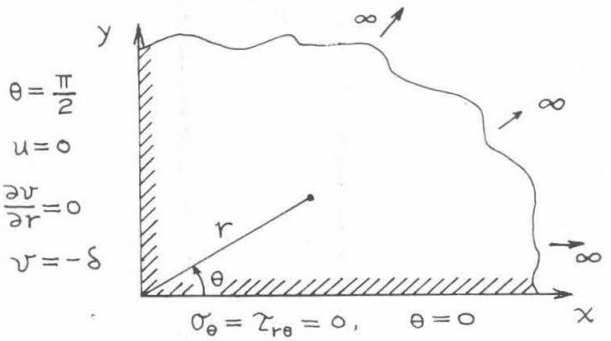

Sketch 1 Clamped-Free Quarter Space

Formally speaking, at $\theta = 0$, the free condition demands that $\sigma_y = \tau_{xy} = 0$, and at $\theta = \frac{\pi}{2}$, the clamped condition demands that $u_y = \frac{\partial u_x}{\partial y} = 0$. The listed boundary condition follow from:

$$\sigma_y = \sigma_r \sin^2\theta + \sigma_\theta \cos^2\theta + \tau_{r\theta} \sin 2\theta = \sigma_\theta\Big|_{\theta=0} \tag{IV. 42}$$

$$\tau_{xy} = \frac{\sigma_r - \sigma_\theta}{2} \sin 2\theta + \tau_{r\theta} \cos 2\theta = \tau_{r\theta}\Big|_{\theta=0} \tag{IV. 43}$$

$$u_y = u \sin\theta + v \cos\theta = u\big|_{\theta=\frac{\pi}{2}} \tag{IV. 44}$$

$$\frac{\partial u_x}{\partial y} = \left(\sin\theta \frac{\partial}{\partial r} + \frac{\cos\theta}{r}\frac{\partial}{\partial\theta}\right)\left(u\cos\theta - v\sin\theta\right) = -\frac{\partial v}{\partial r}\Big|_{\theta=\frac{\pi}{2}} \tag{IV. 45}$$

5. The stresses and displacements in clamped-free quarter space. We rewrite (IV. 41b) as:

$$\Phi = r^{1+n} F(\theta) \qquad \text{, where} \tag{IV. 46}$$

$$F(\theta) = A\sin(1+n)\theta + B\cos(1+n)\theta + C\sin(1-n)\theta + D\cos(1-n)\theta \tag{IV. 47}$$

From (IV. 5) (IV. 6) and (IV. 7) evolve the stresses:

$$\sigma_r = \frac{(1+n)F + F''}{r^{1-n}} \tag{IV. 48}$$

$$\sigma_\theta = \frac{(1+n)nF}{r^{1-n}} \tag{IV. 49}$$

$$\tau_{r\theta} = \frac{-nF'}{r^{1-n}} \tag{IV. 50}$$

Note that if indeed $|n| < 1$, then all the stress components are singular at the corner, and a fortiori, if n is negative. Combining ((IV. 8), (IV. 9), and (IV. 11)) with ((IV. 13), (IV. 14), and (IV. 15)), we obtain:

$$2\mu\frac{\partial u}{\partial r} = \frac{(1+n)\left[1-\sigma(1+n)\right]F + (1-\sigma)F''}{r^{1-n}} \tag{IV. 51}$$

$$2\mu u = \left\{ (1+n)\left[1-\sigma(1+n)\right]F + (1-\sigma)F'' \right\} \frac{r^n}{n} + f(\theta) \qquad \text{(IV. 52)}$$

$$2\mu\left(\frac{u}{r}+\frac{1}{r}\frac{\partial v}{\partial\theta}\right) = -\frac{(1+n)\left[(1+n)\sigma - n\right]F + \sigma F''}{r^{1-n}} \qquad \text{(IV. 53)}$$

$$2\mu\left(u+\frac{\partial v}{\partial\theta}\right) = -\left\{ (1+n)\left[(1+n)\sigma - n\right]F + \sigma F'' \right\} r^n \qquad \text{(IV. 54)}$$

$$2\mu\frac{\partial v}{\partial\theta} = -\frac{(1+n)(1-n^2)(1-\sigma)}{n} r^n F - \frac{1-(1-n)\sigma}{n} r^n F'' - f(\theta) \qquad \text{(IV. 55)}$$

$$2\mu v = -\frac{(1+n)(1-n^2)(1-\sigma)}{n} r^n \int F d\theta - \frac{1-(1-n)\sigma}{n} r^n F' - \int f d\theta + g(r) \qquad \text{(IV. 56)}$$

$$2\mu\frac{\partial v}{\partial r} = -\frac{(1+n)(1-n^2)(1-\sigma)}{r^{1-n}} \int F d\theta - \frac{1-(1-n)\sigma}{r^{1-n}} F' + g' \qquad \text{(IV. 57)}$$

$$2\mu\frac{v}{r} = -\frac{(1+n)(1-n^2)(1-\sigma)}{n\, r^{1-n}} \int F d\theta - \frac{1-(1-n)\sigma}{n\, r^{1-n}} F' - \frac{\int f d\theta}{r} + \frac{g}{r} \qquad \text{(IV. 58)}$$

$$2\mu\left(\frac{\partial v}{\partial r}-\frac{v}{r}\right) = \frac{(1-n^2)^2(1-\sigma)}{n\, r^{1-n}} \int F d\theta + \frac{(1-n)\left[1-(1-n)\sigma\right]}{n\, r^{1-n}} F' + \left(g' - \frac{g}{r}\right) + \frac{\int f d\theta}{r} \qquad \text{(IV. 59)}$$

$$2\mu\left(\frac{1}{r}\frac{\partial u}{\partial\theta}\right) = \frac{(1+n)\left[1-\sigma(1+n)\right]}{n\, r^{1-n}} F' + \frac{1-\sigma}{n r^{1-n}} F''' + \frac{f'}{r} \qquad \text{(IV. 60)}$$

$$2\tau_{r\theta} = -\frac{2nF'}{r^{1-n}} = \frac{(1-n^2)(1-\sigma)}{n\, r^{1-n}} \int F d\theta + \frac{2\left[1-\sigma(1+n^2)\right]}{n\, r^{1-n}} F' + \qquad \text{(IV. 61)}$$
$$+ \frac{1-\sigma}{n r^{1-n}} F''' + \left(g' - \frac{g}{r}\right) + \frac{\int f d\theta + f'}{r}$$

$$0 = \frac{(1-n^2)^2(1-\sigma)}{n\, r^{1-n}} \int F d\theta + \frac{2(1+n^2)(1-\sigma)}{n\, r^{1-n}} F' + \frac{1-\sigma}{n r^{1-n}} F''' \qquad \text{(IV. 62)}$$
$$+ \left(g' - \frac{g}{r}\right) + \frac{\int f d\theta + f'}{r}$$

In (IV. 62) the terms involving F satisfy identically as can be observed by using (IV. 47). It follows that:

$$g = K r \qquad \text{(IV. 63)}$$

$f = I \sin\theta + J \cos\theta$, where I, J, K, are constants. (IV. 64)

From conditions (IV. 42) and (IV. 43) with (IV. 49),(IV. 50) it follows that:

$F(0) = F'(0) = 0$, from which (IV. 65)

$D = -B$ (IV. 66)

$C = -A\left(\frac{1+n}{1-n}\right)$, from which (IV. 67)

$$F(\theta) = A\left[\sin(1+n)\theta - \frac{1+n}{1-n}\sin(1-n)\theta\right] + B\left[\cos(1+n)\theta - \cos(1-n)\theta\right] \qquad \text{(IV. 68)}$$

$$F(\theta) = A(1+n)\left[\cos(1+n)\theta - \cos(1-n)\theta\right] - B\left[(1+n)\sin(1+n)\theta - (1-n)\sin(1-n)\theta\right] \qquad \text{(IV. 69)}$$

$$F''(\theta) = -A(1+n)\left[(1+n)\sin(1+n)\theta - (1-n)\sin(1-n)\theta\right] - \qquad \text{(IV. 70)}$$
$$- B\left[(1+n)^2\cos(1+n)\theta - (1-n)^2\cos(1-n)\theta\right]$$

$$\int F\,d\theta = -A\left[\frac{\cos(1+n)\theta}{1+n} - \frac{(1+n)}{(1-n)^2}\cos(1-n)\theta\right] + B\left[\frac{\sin(1+n)\theta}{1+n} - \frac{\sin(1-n)\theta}{1-n}\right] \qquad \text{(IV. 71)}$$

From conditions (IV. 44) and (IV. 45) with (IV. 52), (IV. 57), (IV. 63), (IV. 64), it follows that

$$f(\theta) = I = J = 0 \qquad \text{(IV. 72)}$$

$$g' = K = 0 \tag{IV. 73}$$

$$F\left(\frac{\pi}{2}\right) = -\frac{2An}{1-n}\cos n\frac{\pi}{2} - 2B\sin n\frac{\pi}{2} \tag{IV. 74}$$

$$F'\left(\frac{\pi}{2}\right) = -2A(1+n)\sin n\frac{\pi}{2} - 2Bn\cos n\frac{\pi}{2} \tag{IV. 75}$$

$$F''\left(\frac{\pi}{2}\right) = -2An(1+n)\cos n\frac{\pi}{2} + 2B(1+n^2)\sin n\frac{\pi}{2} \tag{IV. 76}$$

$$\int_{\frac{\pi}{2}}^{\frac{\pi}{2}} F\,d\theta = \frac{2(1+n^2)}{(1+n)(1-n)^2}A\sin n\frac{\pi}{2} - \frac{2n}{1-n^2}B\cos n\frac{\pi}{2} \tag{IV. 77}$$

$$0 = A(1+n)(2-n-2\sigma)\cos n\frac{\pi}{2} + B(1-n)(1-n-2\sigma)\sin n\frac{\pi}{2} \tag{IV. 78}$$

$$0 = A(1+n)(1+n-2\sigma)\sin n\frac{\pi}{2} - B(1-n)(2+n-2\sigma)\cos n\frac{\pi}{2} \tag{IV. 79}$$

Equations (IV. 78) and (IV. 79) possess a non-trivial solution only if the determinant of the coefficients of A and B is zero. This leads to:

$$\left[4(1-\sigma)^2 - n^2\right]\cos^2 n\frac{\pi}{2} = \left[n^2 - (1-2\sigma)^2\right]\sin^2 n\frac{\pi}{2} \quad \text{, or} \tag{IV. 80}$$

$$1-2\sigma = -\cos^2 n\frac{\pi}{2} + \sqrt{n^2 - \cos^2 n\frac{\pi}{2}\sin^2 n\frac{\pi}{2}} \tag{IV. 81}$$

Figure 1 shows the behavior of the magnitude of the eigenvalue n as a function of Poisson's ratio σ. Note that as $\sigma \to 0$, n must approach and is bounded by unity, whereas when $\sigma \to 1/2$, $n \to \cos n\frac{\pi}{2}$, so that the magnitude of the minimum eigenvalue is 0.595. Since $(1-2\sigma)$ is an even function of n, it

follows that both positive and negative values of the eigenvalue are equally acceptable: we will decide from physical considerations which values are extraneous. Finally observe that, for $\sigma = 1/4$, $n \sim 3/4$, which might be chosen as a typically representative eigenvalue for materials of intermediate dilatancy[1].

From (IV.78) we have:

$$\frac{A}{B} = \frac{1-n}{1+n}\,\frac{n-1+2\sigma}{2-2\sigma-n}\,\tan n\frac{\pi}{2} \quad > 0 \qquad \text{(IV.82)}$$

$$\frac{D}{B} = -1 \qquad \text{(IV.83)}$$

$$\frac{C}{B} = -\frac{n-(1-2\sigma)}{2-2\sigma-n}\tan n\frac{\pi}{2} \quad < 0 \qquad \text{(IV.84)}$$

The stress function can now be written in the following way

$$\Phi = B_n\, r^{n+1}\, F_n(\theta) \qquad \text{(IV.85)}$$

where for each eigenvalue n there exists a constant B_n and a function $F_n(\theta)$. The above expression for Φ is a complimentary solution, potentially complex depending upon the potentially complex nature of the eigenvalues. In order to prescribe a definite tangential displacement

---

(1) Max Knein, Zur Theorie des Druckversuchs. Abhandlungen aus dem Aerodynamischen Institut an der Technischen Hochschule Aachen, Heft 7, 43 (1927)

on the ray $\theta = \pi/2$ a particular solution has to be found which generates this displacement. The unknown coefficients B_n in (IV.85) have to be evaluated by consideration of appropriate boundary conditions along a circumferential arc far from the corner.

Similar arguments apply immediately to the free-free and clamped-clamped spaces. These cases were all discussed by M. L. Williams[2] who, recognized and pointed out that n must be regarded as complex if one is to fit non-trivial boundary conditions. In addition, Williams writes down the general formulae for the eigenvalues in spaces with non-normal corners. Knein restricts his discussion to normal corners.

5. Complex Variable Approach

One of the difficulties inherent in the eigenvalue method restricted to the real domain is that it operates only with one set of a pair of degenerate set of functions which satisfy the biharmonic equation. For the general contour one must use both sets-the circular and the hyperbolic functions. These sets may be combined by the introduction of an appropriate variable.

The apparent difficulty connected with the use of (IV.28) arises from the presence of the logarithmic argument. This however can be disposed of very neatly by mapping the sector of flank angle α (we now generalize to the non-normal corner) onto a strip of width α. This is accomplished by the mapping (cf Sketch 2)

$$\zeta = \ln z \qquad \text{or} \qquad z = e^{\zeta} \tag{IV.86}$$

---

(2) M. L. Williams: Stress Singularities Resulting from Various Boundary Conditions in Angular Corners of Plates in Extension, Journal of Applied Mechanics, 526, (1952)

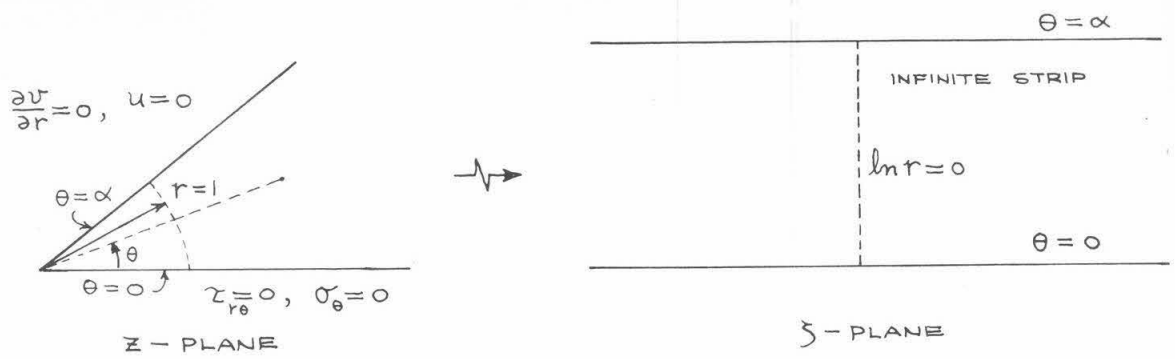

Sketch 2

Note that this mapping allows parallel lines, which replace the rays, to meet at infinity. In order to specify the boundary conditions on the parallel lines, the expressions for the stresses and displacements in terms of complex potentials must be introduced.

The basis for this technique lies in the identification of the geometry of the elastic body with that of the complex plane. This immediately bestows a large number of useful and simplifying features upon the field equation.

The polar plane is related to the complex plane by the analytic mapping:

$$z = re^{i\theta} , \qquad \bar{z} = re^{-i\theta} \tag{IV.87}$$

$$r = \sqrt{z\bar{z}} , \qquad \theta = -i \ln \sqrt{\frac{\bar{z}}{z}} \tag{IV.88}$$

Treating z and $\bar{z}$ as two new independent variables and following the usual rules of calculus of transformation of variables, we can convert the equilibrium equations, and the compatibility equation to the new variables as follows:

$$r \frac{\partial}{\partial r} = z \frac{\partial}{\partial z} + \bar{z} \frac{\partial}{\partial \bar{z}} \tag{IV.89}$$

$$\frac{\partial}{\partial \theta} = iz - i\bar{z} \frac{\partial}{\partial \bar{z}} \tag{IV.90}$$

$$\nabla^2 = 4\frac{\partial^2}{\partial z\, \partial \bar{z}} \tag{IV. 91}$$

Note the elegant form of the Laplacian. Now introduce new stress components and rewrite the equilibrium equations:

$$s = \sigma_r + \sigma_\theta \tag{IV. 92}$$

$$t = \frac{\sigma_r - \sigma_\theta}{2} + i\,\tau_{r\theta} \tag{IV. 93}$$

$$\bar{t} = \frac{\sigma_r - \sigma_\theta}{2} - i\,\tau_{r\theta} \tag{IV. 94}$$

$$\bar{z}\, s_{\bar{z}} + 2t + 2z\, t_z = 0 \tag{IV. 95}$$

$$z\, s_z + 2\bar{t} + 2\bar{z}\, \bar{t}_{\bar{z}} = 0 \tag{IV. 96}$$

Now introduce the stress function:

$$s = \nabla^2 \Phi = 4\, \Phi_{z\bar{z}} \tag{IV. 97}$$

$$\bar{t} = -2\frac{z}{\bar{z}}\, \Phi_{zz} \tag{IV. 98}$$

$$t = -2\frac{\bar{z}}{z} \Phi_{\bar{z}\bar{z}} \tag{IV. 99}$$

New strains are introduced and then Hooke's Law:

$$\vartheta = \epsilon_r + \epsilon_\theta \tag{IV.100}$$

$$\gamma = \frac{\epsilon_r - \epsilon_\theta}{2} + i\epsilon_{r\theta} \tag{IV.101}$$

$$\overline{\gamma} = \frac{\epsilon_r - \epsilon_\theta}{2} - i\epsilon_{r\theta} \tag{IV.102}$$

$$2\mu\vartheta = (1-2\sigma)\, s \tag{IV.103}$$

$$2\mu\gamma = t \tag{IV.104}$$

$$2\mu\overline{\gamma} = \overline{t} \tag{IV.105}$$

New displacements are introduced and related to the strains:

$$u = u_r + i\, u_\theta \tag{IV.106}$$

$$\overline{u} = u_r - i\, u_\theta \tag{IV.107}$$

$$\vartheta = \frac{\frac{u+\overline{u}}{2} + z\,u_z + \overline{z}\,\overline{u}_{\overline{z}}}{\sqrt{z\overline{z}}} \tag{IV.108}$$

$$\gamma = \frac{\overline{z}\,u_{\overline{z}} - u/2}{\sqrt{z\overline{z}}} \tag{IV.109}$$

$$\overline{\gamma} = \frac{z\,\overline{u}_z - \overline{u}/2}{\sqrt{z\overline{z}}} \tag{IV.110}$$

Elimination of u and $\overline{u}$ from (IV.108), (IV.109), (IV.110) establishes compatibility:

$$z\overline{z}\,\vartheta_{z\overline{z}} = z^2\gamma_{zz} + 2z\,\gamma_z + \overline{z}^2\overline{\gamma}_{\overline{z}\overline{z}} + 2\overline{z}\,\overline{\gamma}_{\overline{z}} \tag{IV.111}$$

Introduction of the stresses from (IV. 103), (IV. 104), (IV. 105) and then the stress function from (IV. 97), (IV. 98), (IV. 99) establishes the biharmonic character of Φ :

$$\Phi_{zz\bar{z}\bar{z}} = 0 \tag{IV. 112}$$

In a purely formal fashion, if Φ is assumed to be analytic, (IV. 112) can be integrated to express Φ in terms of two arbitrary holomorphic functions ϕ and χ, both of which must be harmonic:

$$2\Phi = \bar{z}\phi + z\phi + \chi + \overline{\chi} \tag{IV. 113}$$

The derivatives are useful

$$2\Phi_z = \bar{z}\phi_z + \overline{\phi} + \chi_z \tag{IV. 114}$$

$$2\Phi_{\bar{z}} = z\overline{\phi}_{\bar{z}} + \phi + \overline{\chi}_{\bar{z}} \tag{IV. 115}$$

$$2\phi_{z\bar{z}} = \phi_z + \overline{\phi}_{\bar{z}} \tag{IV. 116}$$

Note that $\phi = \phi(z)$ depends only on z and so has no derivative with respect to $\bar{z}$. This is significance of harmonic behavior. Note also that

$$\overline{\phi}(\bar{z}) \neq \phi(z) \tag{IV. 117}$$

since ϕ may be a complex function.

The stress and displacements may be expressed in terms of ϕ and χ.

$$s = 2(\phi_z + \overline{\phi}_{\bar{z}}) \tag{IV. 118}$$

$$t = -z\phi_{zz} - \frac{z}{\bar{z}}\chi_{zz} \tag{IV. 119}$$

$$\overline{t} = -\bar{z}\overline{\phi}_{\bar{z}\bar{z}} - \frac{z}{\bar{z}}\overline{\chi}_{\bar{z}\bar{z}} \tag{IV. 120}$$

$$2\mu u = (3-4\sigma)\sqrt{\frac{z}{\bar{z}}}\,\phi - \sqrt{z\bar{z}}\,(\bar{\phi}_{\bar{z}} + iC) - \sqrt{\frac{z}{\bar{z}}}\,(\bar{\chi}_{\bar{z}} + B) \qquad \text{(IV. 121)}$$

$$2\mu \bar{u} = (3-4\sigma)\sqrt{\frac{\bar{z}}{z}}\,\bar{\phi} - \sqrt{z\bar{z}}\,(\phi_z - iC) - \sqrt{\frac{\bar{z}}{z}}\,(\chi_z + B) \qquad \text{(IV. 122)}$$

Remembering that $z\bar{z} = r$, it is readily observed that C generates a pure totation and B a linear displacement along the x-axis. Thus B and C may be set equal to zero with no loss of generality.

6. Boundary conditions in the Complex Plane

From (IV. 92), (IV. 93), and (IV. 94), we have:

$$s + t + \bar{t} = 2\sigma_\theta = 0 \qquad \text{at} \qquad \theta = 0 \qquad \text{(IV. 123)}$$

$$t - \bar{t} = 2i\tau_{r\theta} = 0 \qquad \text{at} \qquad \theta = 0 \qquad \text{(IV. 124)}$$

Therefore t must be real.

Along the other ray, we have from (IV. 106), and (IV. 107)

$$u + \bar{u} = 2u_r = 0 \qquad \text{at} \qquad \theta = \alpha \qquad \text{(IV. 125)}$$

Therefore u must be imaginary. Also from (IV. 89) we have:

$$\left.\frac{\partial u}{\partial r}\right|_{\theta=\alpha} = \left(\sqrt{\frac{z}{\bar{z}}}\,\frac{\partial}{\partial z} + \sqrt{\frac{\bar{z}}{z}}\,\frac{\partial}{\partial \bar{z}}\right)(u - \bar{u}) = 0 \qquad \text{which becomes:} \qquad \text{(IV. 126)}$$

$$z u_z + \bar{z} u_{\bar{z}} = z\bar{u}_z + \bar{z}\bar{u}_{\bar{z}} \qquad \text{(IV. 127)}$$

The problem now is to choose ϕ or $\bar{\phi}$ and χ so as to most conveniently fit these boundary conditions. In addition to the set (IV. 123), - (IV. 127) we shall expect to impose some restriction, at $r \to \infty$, that either the stresses or displacements go to zero.

As already indicated, the problem of choosing is tremendously simplified by mapping the sector onto an infinite strip. This transformation introduces new variables:

$$\zeta = \ln z \,, \qquad \bar{\zeta} = \ln \bar{z} \tag{IV. 128}$$

$$z = e^{\zeta} \,, \qquad \bar{z} = e^{\bar{\zeta}} \tag{IV. 129}$$

$$\frac{\partial}{\partial z} = e^{-\zeta} \frac{\partial}{\partial \zeta} \tag{IV. 130}$$

$$\frac{\partial}{\partial \bar{z}} = e^{-\bar{\zeta}} \frac{\partial}{\partial \bar{\zeta}} \tag{IV. 131}$$

so that the Laplacian becomes:

$$\nabla^2 = 4 e^{-(\zeta+\bar{\zeta})} \frac{\partial^2}{\partial \zeta \partial \bar{\zeta}} \tag{IV. 132}$$

The biharmonic loses its simple one-term character:

$$\Phi_{\zeta\zeta\bar{\zeta}\bar{\zeta}} - \Phi_{\zeta\zeta\bar{\zeta}} - \Phi_{\zeta\bar{\zeta}\bar{\zeta}} + \Phi_{\zeta\bar{\zeta}} = 0 \tag{IV. 133}$$

And the complex stresses, displacements and potentials become

$$2\Phi = e^{\bar{\zeta}}\phi + e^{\zeta}\bar{\phi} + \chi + \bar{\chi} \tag{IV. 134}$$

$$s = 2\left(e^{-\zeta}\phi_{\zeta} + e^{-\bar{\zeta}}\bar{\phi}_{\bar{\zeta}}\right) \tag{IV. 135}$$

$$t = e^{-\bar{\zeta}}\left(\bar{\phi}_{\bar{\zeta}} - \bar{\phi}_{\bar{\zeta}\bar{\zeta}}\right) + e^{-(\zeta+\bar{\zeta})}\left(\bar{\chi}_{\bar{\zeta}} - \bar{\chi}_{\bar{\zeta}\bar{\zeta}}\right) \tag{IV. 136}$$

$$2\mu u = \left[(3-4\sigma)\phi - \bar{\chi}_{\bar{\zeta}}\right] e^{-\left(\frac{\zeta-\bar{\zeta}}{2}\right)} - \bar{\phi}_{\bar{\zeta}} e^{\frac{\zeta-\bar{\zeta}}{2}} \tag{IV. 137}$$

On the boundaries of the strip, we now have

$$\text{at} \quad \zeta = \bar{\zeta} \,, \quad \frac{s}{2} = t = \bar{t} \tag{IV. 138}$$

$$\text{at} \quad \zeta - \bar{\zeta} = 2i\alpha, \quad u = -\delta e^{-i\alpha}, \quad u_\zeta + u_{\bar{\zeta}} = 0 \tag{IV. 139}$$

Equations (IV. 138) and (IV. 139) may be solved by first taking Fourier transforms and then solving a pair of simultaneous algebraic equations and then inverting the Fourier integrals. The exact details of this procedure are being worked out and will be reported in the next monthly report. In addition, the sector-space will also be mapped onto a half-plane by the mapping

$$\zeta = z^{\frac{\pi}{2}} \tag{IV. 140}$$

This reduces the integral equations to a Hilbert problem, which will be discussed in detail in the subsequent report.

FIG. IV. 1. DEPENDENCE OF EIGENVALUE ON POISSON'S RATIO